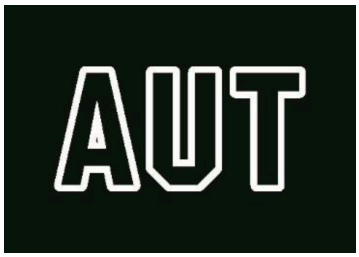

School of Science

The Synthesis of Phenol Glycosides as Markers for Smoke Taint in Wine

Shaun D'souza

ID : 18018667

A dissertation submitted in partial fulfilment

of the requirements for the degree of

Bachelor of Advanced Science (Honours)

Auckland University of Technology

30th November 2022

Abstract

Wildfires can cause a number of different issues for the winemaker such as damages to crops and property, with the biggest issue being economic losses due to smoke-tainted wine. This project looked into finding a lasting solution to the problem of smoke-tainted wine. The main aim of this project was to synthesise the novel phenolic glycoside, para-cresol gentiobioside, which is one on many compounds that are responsible for smoke taint in wine. The compound, when synthesised will then be used by the industrial collaborators involved in this project to develop molecularly imprinted polymers to selectively remove the same or other closely-related compounds. All reactions in the proposed synthetic scheme for para-cresol gentiobioside were performed and were also optimised where necessary to obtain a better yield at that step. 0.0750 grams of the novel compound, para-cresol gentiobioside was successfully synthesised in this project. In the final stages of the project an alternative synthetic route which was more efficient and which could potentially provide faster access to other phenolic glycosides responsible for smoke taint was explored.

Table of Contents

Abbreviations

MIP -	Molecularly Imprinted Polymers
S_N1 -	Unimolecular Nucleophilic Substitution
S_N2 -	Bimolecular Nucleophilic Substitution
$AgClO_4$ -	Silver perchlorate
AgOTf -	Silver triflate
$AgNO_3$ -	Silver nitrate
Ag_2CO_3 -	Silver carbonate
Ag_2O -	Silver oxide
$HgBr_2$ -	Mercury (II) bromide
HgI_2 -	Mercury (II) iodide
$CHCl_3$ -	Chloroform
Et_3N -	Triethylamine
NMR -	Nuclear Magnetic Resonance
^1H NMR -	Proton Nuclear Magnetic Resonance
^{13}C NMR -	Carbon-13 Nuclear Magnetic Resonance
COSY -	^1H-^1H Correlation Spectroscopy
HSQC -	Heteronuclear Single-Quantum Coherence Spectroscopy
$BF_3.OEt_2$ -	Boron trifluoride etherate
DCM -	Dichloromethane
$NaHCO_3$ -	Sodium bicarbonate
EtOAc -	Ethyl acetate
MeOH -	Methanol
H_2O -	Water
DMAP -	4-Diemthylaminopyridine
TLC -	Thin Layer Chromatography
IR -	Infra-red
AcOH -	Acetic acid
Ph_3CCl -	Trityl chloride
$MgSO_4$ -	Magnesium sulphate
HCl -	Hydrogen Chloride

List of figures

Attestation of Authorship

I hereby declare that this submission is my own work and that, to the best of my knowledge and belief, it contains no material previously published or written by another person (expect where explicitly defined in the acknowledgements), nor material which to a substantial extent has been submitted for the award of any other degree or diploma of a university or other institution of higher learning.

Shaun D'souza
30th November 2022

Acknowledgements

I would like to express my gratitude to the following individuals, without the help of whom I could not have completed this research and would not have successfully completed my honour's year.
Firstly, A big thank you my supervisor, Dr. Jack Chen, for his exemplary guidance, valuable feedback and constant encouragement throughout the duration of the project. His valuable suggestions were of immense help throughout my project. Working under him was an extremely knowledgeable experience for me. Lastly, a special thank you to Dr. Mohinder Naiya, who provided insight and expertise that greatly assisted me throughout the course of this project.

CHAPTER ONE : INTRODUCTION

1.1 Smoke Tainted Wine

Wildfires are a major climate issue all over the world, with consequences for public safety and land use. In recent years, wildfires have not only become more frequent and severe in areas that are prone to them, but they have also started to spread to new areas.[1] Every year, almost 350 million hectares of land are burned worldwide.[1] According to the 2019 annual global climate record by the National Oceanic and Atmospheric Administration, the last 15 years have been the warmest years on record, out of which the year 2016 had the highest global surface temperature to date, which measured 0.99 °C above average.[1] Climate change is widely acknowledged to be a factor in the increased incidence of fire incidents worldwide, which is exacerbated by a number of other factors, such as hotter, drier, and windy weather conditions; lower rainfall levels, which cause prolonged droughts; and much higher fuel loads, which depend on how land and fire are managed.[2] Climate pressures are affecting a lot of the world's most prominent wine regions, including those in Australia, the United States, South Africa, Chile, and Canada, and wildfires have created serious problems for the wine industry, including damages to vineyards and crop loss as a result of burning or smoke exposure.[3] Wildfires are expected to become more frequent and severe as climate change continues, affecting winemaking areas that have not yet been seriously affected.[3] Though wildfires can cause a number of different issues for the winemaker such as damages to crops, property and economic losses due to smoke taint, this project will look specifically into the problem of smoke tainted wine.[3]

When exposed to smoke, grapevine leaves and fruit can absorb volatile smoke compounds.[4]Examples of such compounds include volatile phenols such as ortho-, meta- and para-cresol, syringol, guaiacol, and 4-methylguaiacol.[4] Figure 1 below shows the chemical structures of these volatile smoke compounds.

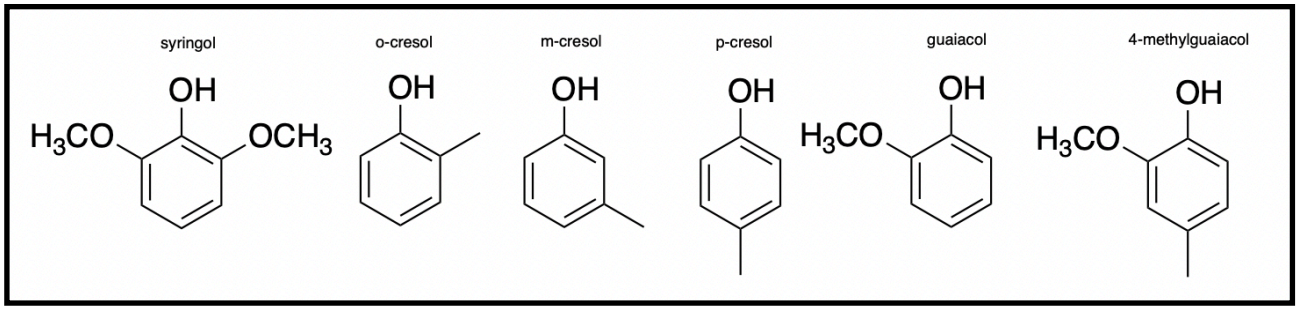

Figure 1 - Chemical structures of some volatile smoke compounds

Detected initially in their free (aglycone) forms, these volatile compounds are then quickly converted to a much stable glycoconjugate form via glycosylation, which in this case is an O-glycosylation.[4] Figure 2 below shows the chemical structure of syringol gentiobioside, an example of a glycosylated form of the volatile smoke compound syringol, which was shown previously in figure 1.

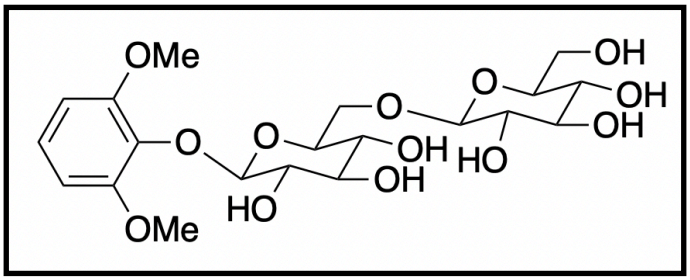

Figure 2 - Chemical structure of syringol gentiobioside

During the fermentation process, these glycoconjugates are then broken down and the volatile phenols are liberated, which in turn results in undesirable sensory characters in the resulting wine.[4] These undesirable sensory characters present in smoke tainted wine are commonly described as being smoky, ashy, burnt, medicinal, burnt rubber and earthy.[4] Therefore as a result of these undesirable sensory characters, such smoke tainted wine is no longer marketable and is by far the biggest commercial damage to the winemaker.[5] As an example, the north-east Victorian wine industry was estimated to have lost $4 million due to smoke damage and quality loss in wines as a result of the 2003 Canberra bushfires. Till date the exact pathway by which these volatile smoke compounds are taken up has not yet been determined.[6] In one particular isotope tracing experiment carried out by Hayasaka et al. (2010), it was found that the translocation of these compounds, in both their glycoconjugate and aglycone forms, was minimal between different parts of the grapevine.[6] However in another study carried out by Kennison et al. (2009), wines made from grapes that were exposed to smoke for just 30 minutes during the growing season exhibited elevated phenol levels.[7] Therefore, it is likely that there is some pathway by which these volatile smoke compounds are absorbed directly and instantly into the grapevine leaves and fruit. When it comes to the taint found in wines made from smoke-affected grapes, it is still unclear which volatile compounds derived from smoke are to blame.[8] This is because the variety of compounds that contribute to smoke taint may be enormous and complex.[8] As a result of guaiacol and 4-methylguaiacol being frequently found in wines aged in oak barrels, these compounds have been measured in early studies as indicators of smoke taint.[9] The compounds guaiacol and 4-methylguaiacol were known to give oak-aged wines subtle smoky aromas and flavours, with their contribution to wine being viewed favourably in general.[9] With the advancement of smoke taint research, the cresols, phenols, and syringols were eventually added to the list of compounds that were measured as smoke taint markers.[10] In addition to that, various different analytical methods were also developed to measure both the free and glycosylated forms of these volatile phenols.[10]

As smoke taint research progresses, it is reasonable to anticipate that additional smoke taint marker compounds will likely be discovered in the future.[10] When it comes to reducing and/or reversing the effects of grapevine smoke exposure, a number of different techniques have been examined, including preventative viticultural practises and ameliorative winemaking techniques.[1] However as of now, there is no single technique available that is known to completely eliminate the effects of smoke taint in wine.[1] Therefore, the main focus of this project was to look into a lasting solution to the problem of smoke taint in wine. The proposed solution was understood to be a very unique and highly efficient way of using molecularly imprinted polymers to selectively remove all compounds responsible for the presence of smoke taint in wine.

1.2 Molecularly Imprinted Polymers

Molecular imprinting is a method for creating highly cross-linked polymers that can recognise specific molecules.[11] Figure 3 shown below summarises this principle where interacting and cross linking monomers are arranged around a molecular template, then polymerisation occurs to create a cast-like shell.[12]

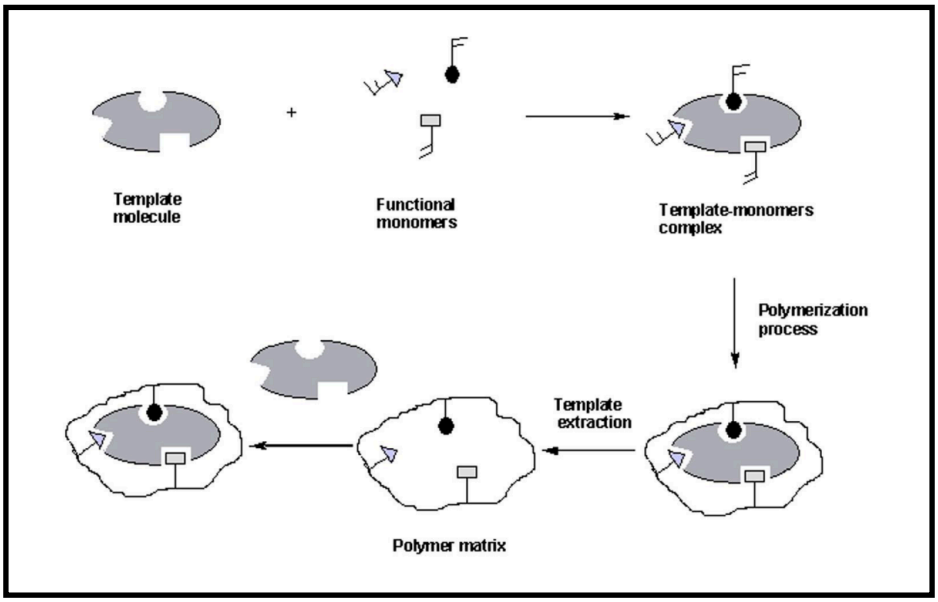

Figure 3 - Summary of the molecular imprinting process

Dissolution of the template, functional monomer, cross linking agent, and initiator in a pyrogenic solvent is the first step in the process.[12] Since the formation of a stable template-monomer complex is essential for the success of molecular recognition, functional monomers are chosen to interact with the template molecule.[11] In the next step, by copolymerising with cross linking monomers, the position of the monomers around the template is fixed. Moving on, the resulting polymer has a macroporous matrix with microcavities and a complementary three-dimensional structure to the template.[12]

As a result, when the template molecules are removed from the polymer by washing with a solvent, binding sites that are complementary to the template in terms of size, shape, and chemical functionality are left behind.[11] Essentially, the polymer is said to be imprinted with a molecular memory that enables it to to rebind with the target (the template) with precision.[11] The molecular recognition phenomenon is typically driven by intermolecular interactions such as hydrogen bonds, dipole-dipole interactions, and ionic interactions between the template molecule and functional groups present in the polymer matrix.[12] As a result, the finished polymer recognises and binds to the template molecules only. Depending on the interactions created during polymerisation, the binding sites exhibit a variety of characteristics.[12] Historically, molecular imprinting has been categorised based on the type of interactions that occur between the monomer and template during polymerisation.[12]

Molecularly imprinted polymers (MIPs) have a high level of selectivity and affinity for the target molecule used in the imprinting process as their main benefits.[12] In addition to that, when compared to biological systems such as nuclei acids and proteins, these imprinted polymers are known to be stronger, more robust, more resistant towards elevated temperature and pressures levels, and also display inertness towards organic solvents, acids, bases, and metal ions.[12] To add onto that, these molecularly imprinted polymers are also less expensive to produce, and the polymers can retain their molecular memory for several years at room temperature due to their long storage lives.[12] Initially used only as specific separation materials, such as for the chromatographic separation of enantiomers, these molecularly imprinted polymers were first described by Wulff and Mosbach in the 1970s and early 1980s.[13] The great potential of MIPs as synthetic antibody mimics, however, was not realised until the year 1993.[13] Based on these MIP's ability to specifically recognise molecular targets, a number of potential application fields have been identified, including affinity separation, chemical sensors and assays, enzyme-like catalysis and directed synthesis, and also biomedical applications like drug delivery.[13] Till date Analytical chemistry remains the primary application area, and for the past ten years, the only commercially available MIPs for sample preparation and analyte pre-concentration, primarily for biomedical and food analyses, have been solid-phase extraction matrices.[13]

1.3 The Project

The main aim of this project was to synthesise the novel phenol glycoside, para-cresol gentiobioside, which is also a glycosylated form of the volatile smoke compound para-cresol. Figure 4 below shows the proposed synthetic pathway for the synthesis of para-cresol gentiobioside. On completion of the synthesis, the final pure product will be utilised by the industrial collaborators involved in this project to successfully develop molecularly imprinted polymers that will be used to selectively remove the same compound (para-cresol gentiobioside) and other closely related analogues from smoke-tainted wine. Additionally, the final pure product can also be used as a highly effective standard to evaluate the performance of all currently existing molecularly imprinted polymers.

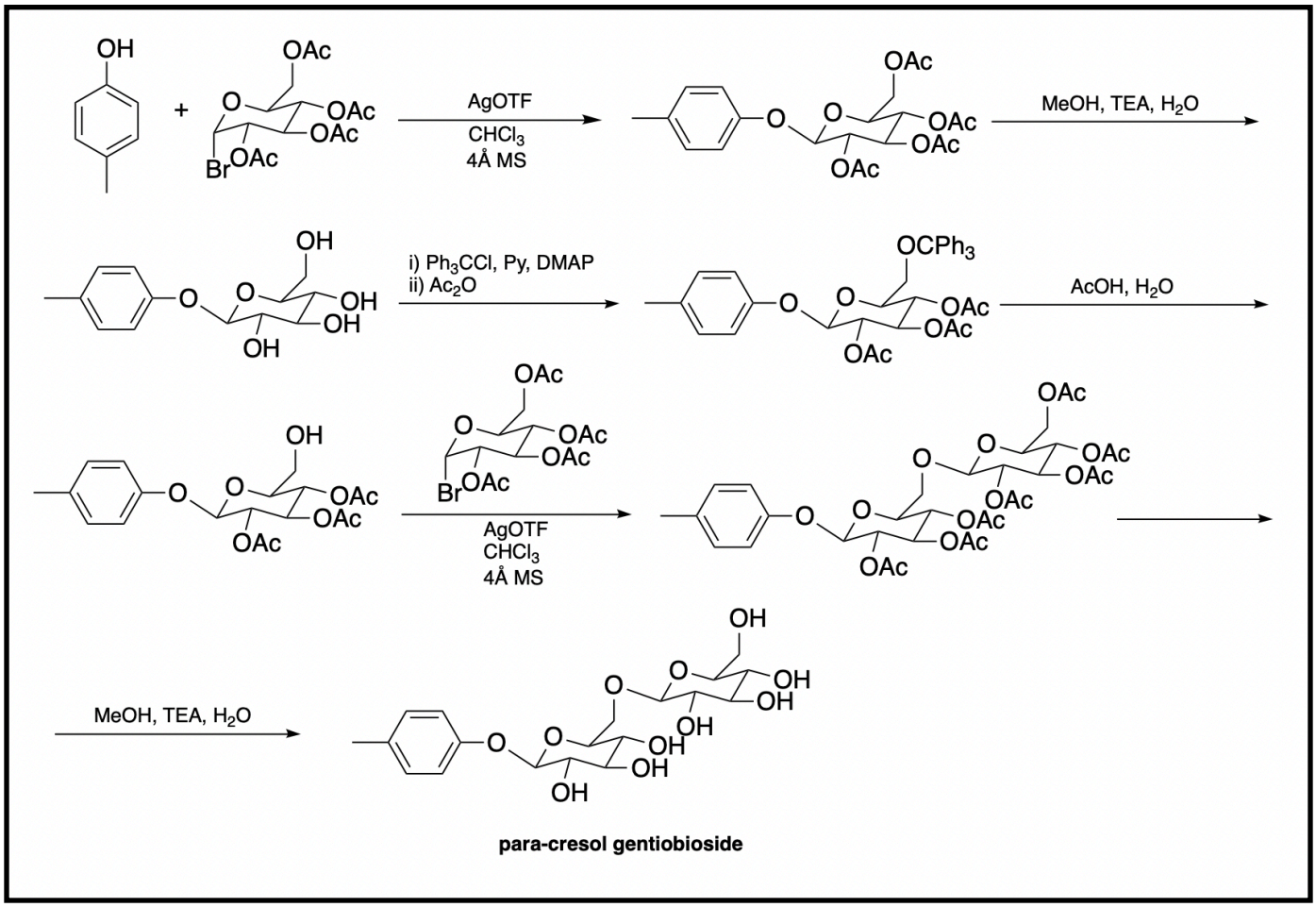

Figure 4 - The proposed synthetic scheme for para-cresol gentiobioside

1.4 Carbohydrate Chemistry

The largest class of naturally occurring compounds are carbohydrates, which can be found as polysaccharides or glycoconjugates.[14] It was previously believed that the structural and protective components in plant, bacterial, and animal cell walls were the only roles they played besides serving as energy-storage components.[15] However, only in the latter half of the 20th century did it become clear that carbohydrates were involved in a variety of other biological processes.[16] Glycoconjugates have immense importance in many biochemical processes, including molecular recognition, transmission of biological information, immunological recognition, cell-cell interaction and so forth, as demonstrated by the renaissance in glycobiology that has occurred over the past few years.[17] The vast majority of carbohydrates found in nature do not exist in a free state, but rather are joined by glycosidic bonds to other monosaccharides or to other types of compounds (aglycones).[18] In nature, it is possible to find compounds with O-, S-, or N-glycosidic linkages, out of which the compounds with O-glycosdic linkages are understood to be the most common and therefore most important.[18] Figure 5 below shows the general structures of O-, S-, and N-glycosides.

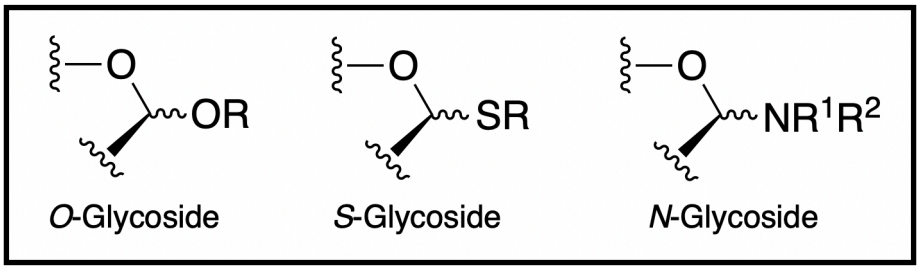

Figure 5 - The general structures of the different glycosides present in nature

In certain situations it may be challenging and time-consuming to isolate complex pure carbohydrate samples (e.g. the phenolic glycosides in this project) in large enough quantities.[14] Therefore in such situations, chemical syntheses aimed at developing these complex carbohydrates becomes crucial.[14] Moving on when developing such compounds, the formation of the glycosidic bond will always be the most important step/steps in the synthesis.[14] Being the most reactive of a monosaccharide's various functional groups, the anomeric centre almost always needs to be temporarily protected during the carbohydrate synthesis process to allow for other positions to undergo chemical changes.[19] The creation of the simple glycoside for momentary anomeric centre protection is very commonly an initial step in multiple step syntheses for carbohydrates.[19] In model compounds, fixing the anomeric configuration as a glycoside is helpful in order to fix any variabilities that results due to the equilibrium of free sugars into various ring sizes and anomeric configurations.[19] Above all, the development of straightforward, efficient, and glycosidic linkages that are stereoselective remains a major challenge for both organic and bio-organic chemistry.[20]

Contrary to peptide syntheses, glycosylation reactions necessitate strict control of stereochemistry.[20] To add onto that, minor changes in the glycosyl donor and acceptor structures could be problematic as the final stereochemistry of the reaction is sensitive to a number of different factors.[21] As a result, understanding these influences and creating more effective and widely applicable glycosylation reactions have long been major challenges for mainstream organic chemistry as well as carbohydrate chemistry.[20]

As it is seen in the synthetic scheme for this project in section 1.3, the main chemistry carried out in this project involved chemical glycosylations and by that the *O*-glycosylations. Therefore it was necessary to get an in-depth understanding of chemical glycosylations. In a chemical glycosylation reaction, a glycosyl donor and a glycosyl acceptor are coupled to form a glycoside.[14] Since Michael and Emil Fischer's first historically significant glycoside syntheses which resulted in the formation of the first aryl and alkyl glycoside bonds, which was then followed by Koenigs and Knorr's ground-breaking work, there have been so many different methods for glycosylation that have been introduced.[21] Among these various glycosylation techniques, nucleophilic substitution reactions at the most reactive carbon centre, the anomeric carbon, account for the vast majority of reactions.[21] Figure 6 below shows the general reaction for *O*-glycoside synthesis where the anomeric carbon is involved in a nucleophilic substitution reaction.

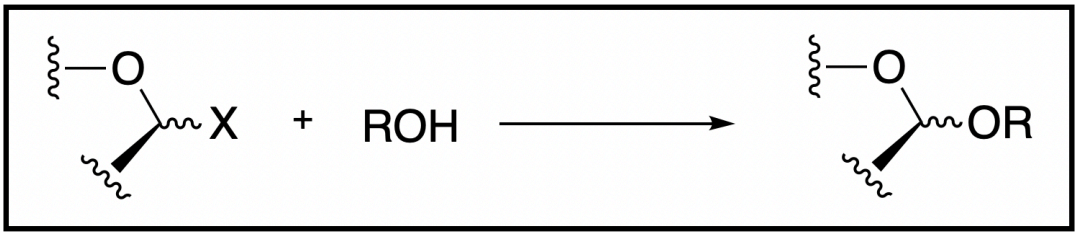

Figure 6 - General reaction of glycoside synthesis

One of the biggest problems in carrying out glycosylation reactions, is ensuring that the final glycoside formed has the right, desired stereochemistry at the anomeric centre.[22] These issues in the stereoselectivity can simply be explained with the help of the mechanism for O-glycoside synthesis.[22] In the mechanism due to the ring oxygen's involvement in nucleophilic displacements, the reaction becomes more S_N1 like instead of S_N2. Therefore as a result of being unable to have a proper S_N2 like mechanism, the resulting glycoside, depending on which side the nucleophile attacks from can be of two types, which are the 1,2-trans glycosides or the 1,2-cis glycosides. Figure 7 on the following page, as an example, shows the general chemical structures of both the 1,2-trans and and the 1,2-cis glycosides for the simple sugar D-glucose, which are also known as the β-anomer and the α-anomer respectively.

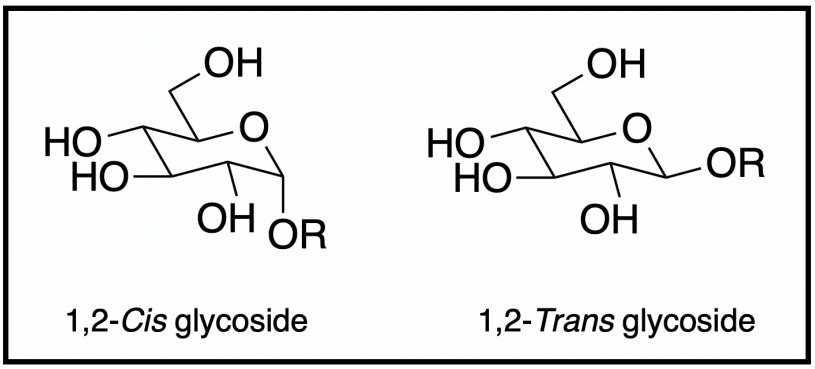

Figure 7 - The General chemical structures of the 1,2-*Cis* and the 1,2-*Trans* glycosides of D-glucose

Although these reactions are difficult to control, on the instance where one would require a proper stereoselective synthesis of only the 1,2-*trans* glycoside, this can be achieved by one particular method which uses neighbouring group participation.[23] Figure 8 shown below shows the overall mechanism of the synthesis of both the 1,2-*trans* and 1,2-*cis* glycosides. Additionally, the mechanism also shows how neighbouring group participation can be used to control the stereoselectivity of the reaction to obtain the 1,2-*trans* glycoside as the major product.

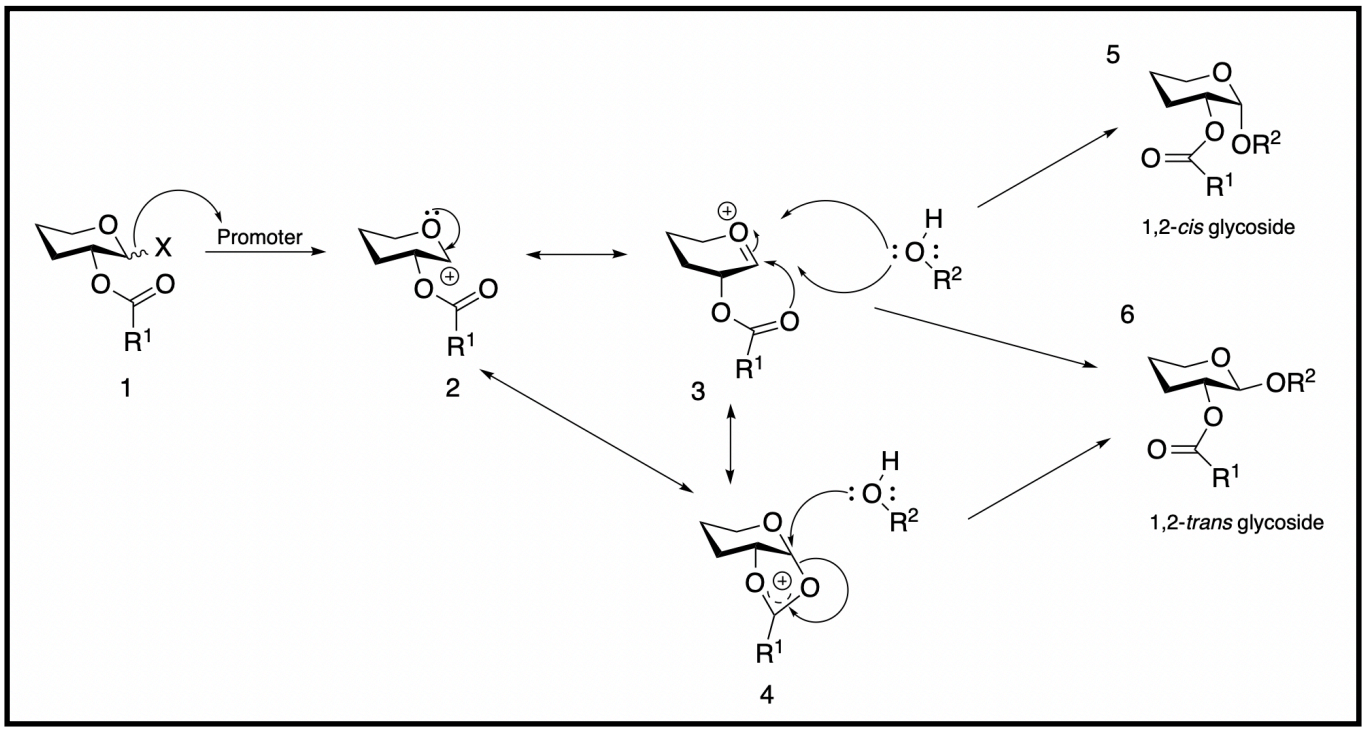

Figure 8 - The mechanism of the 1,2-*cis* and the 1,2-*trans* glycoside formation

The mechanism shown above begins with the removal of the leaving group X from the glycosyl donor (structure 1), which was initiated by the action of a promoter. This then leads to the formation of the carbocation shown in structure 2. In the next step, the donation of the lone pair from the ring oxygen then results in the formation of the oxocarbenium ion shown in structure 3. [23]As a result of the nucleophile being able to attack from two possible faces, it is possible to form both the 1,2-*trans* and the 1,2-*cis* isomer of the glycoside.[23]

However on the instance where there is neighbouring group active substituent on the adjacent carbon, the reaction follows a different pathway. Acyloxy groups are the most notable examples of such neighbouring group active substituents.[24] In the presence of such a group on the adjacent carbon, there is movement of electrons from the carbonyl oxygen onto the anomeric carbon, which then results in the formation of the acyloxonium ion shown in structure 4. This formation of the acyloxonium ion is understood to occur at a faster rate in the presence of a neighbouring group active substituent.[24] Now, as a result of one face (the bottom face) of the glycosyl donor being completely blocked, the nucleophile can only attack the anomeric carbon from the only other available face (the upper face).[14] This then results in the formation of only the 1,2-trans glycoside as shown in structure 6. Therefore from what was discussed above, the use of neighbouring group participation is a very useful way to control the stereochemistry of a glycosylation reaction and get the 1,2-*trans* product of the glycoside exclusively.[14] Substituents such as O-acetyl, O-pivaloyl, and O-benzoyl are some of the most commonly used neighbouring group active substituents.[21]

Moving on, in the instance where one would want to control the stereochemistry of the reaction to get the 1,2-*cis* isomer as the major product, the easiest starting point would be to have substituents on the adjacent carbon that are non-neighbouring group active.[25] Protecting groups that are ether-based are a notable example for such groups.[25] However it is important to note that the use of protecting groups that are non-neighbouring group active alone is not sufficient to achieve full control of the stereochemistry of the reaction. This is because, as mentioned before, regardless of the type of protecting groups used, these reactions still have a considerable S_N1 like character which would still allow for nucleophilic attack from two different planes. Despite there being significant advancements in the synthesis of 1,2-*cis* glycosides, a successful direct method for their preparation has not yet been discovered.[26] This by no means implies that these compounds cannot be accessed synthetically but means that carrying out such syntheses would often call for in-depth knowledge and methodical research. There are however, a number of alternate indirect methods for the synthesis of *cis*-glycosides.[27] The common principle in all those methods was to first utilise neighbouring group participation to get exclusively the *trans*-glycoside, which was then followed by carrying out an inversion at the C-2 carbon which will then create the *cis*-glycoside.[27] Figure 9 on the next page shows an example of a synthetic scheme that follows the above method. In the synthetic scheme, the trans-glycoside formed in the first step had a selectively removable O-Acetyl protecting group at O-2. After this protecting group was removed, the resulting compounds configuration at the C-2 carbon was then inverted by the help of a nucleophilic displacement or redox reaction, which then yields the *cis*-glycoside. [25]However it is important to note that although the compound formed here is a *cis*-glycoside (the -OH group on C-1 is cis with respect to the -OH group on C-2), it is not considered to be an α-glycoside, as in order to be an α-glycoside the -OH group on the C-1 carbon needs to be in an axial position regardless of what position the -OH group on the C-2 carbon is in.[26] Hence, the final glycoside in this reaction is a β-D-mannopyranoside.

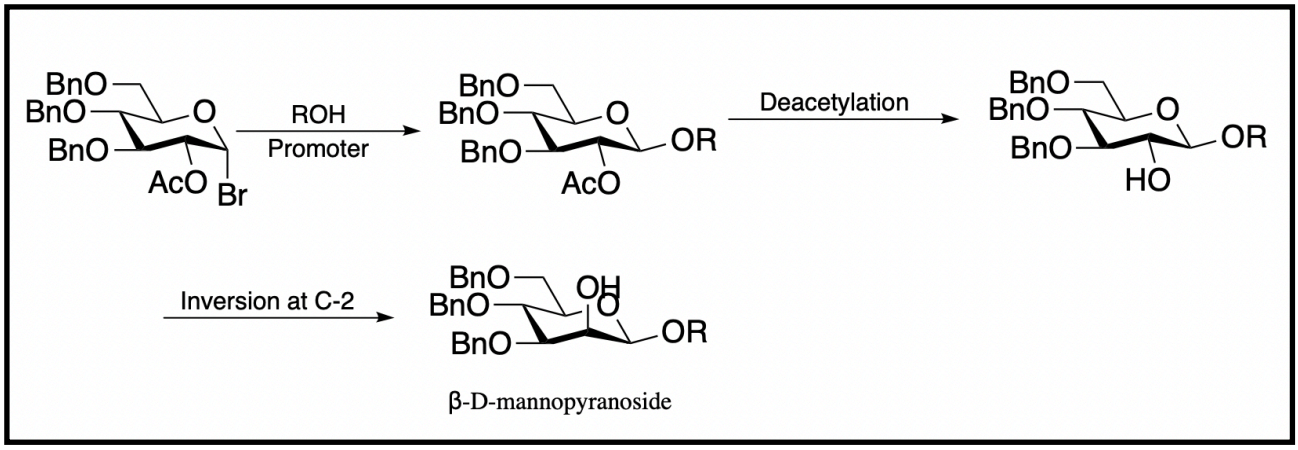

Figure 9 - An indirect route to obtain the *cis*-glycoside

Moving on, based on the type of glycosyl donor that was used, glycoside synthesis can be carried out by a number of different ways.[21] Some of the most common classes of glycoside donors that are used include the glycosyl halides, glycosyl imidates, thioglycosides, and also glycosyl esters.[21]Since the only type of glycosyl donors used in this project were the glycosyl bromides (glycosyl halides), it was necessary to get a better understanding of techniques involving such glycosyl donors. Koenigs and Knorr introduced the use of the glycosyl bromide or chloride as an efficient glycosyl donor in glycosylation reactions in 1901.[29] This well known glycosylation technique, known as the Koenigs-Knorr glycosylation commonly involved the usage of heavy metal salts which acted as promoters or activating reagents in the reaction.[21] $AgClO_4$, AgOTf, $AgNO_3$, Ag_2CO_3, Ag_2O, $HgBr_2$, and HgI_2 are just a few examples of some heavy metal salts that were used in this area.[21] It is also well known that such reactions are very sensitive to moisture and would often require the use of molecular sieves or Drierite to remove water.[21] Figure 10 below shows the overall general reaction of a Koenigs-Knorr glycosylation. The synthetic pathway for the synthesis of para-cresol gentiobioside, the target molecule in this project, involves carrying out two such Koenigs-Knorr O-glycosylation reactions. These reactions will be seen shortly in section 2.1.

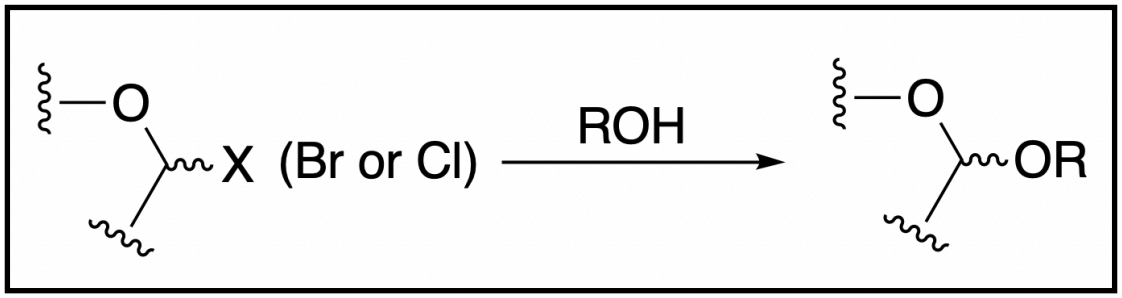

Figure 10 - General reaction of a Koenigs-Knorr glycosylation

CHAPTER TWO : RESULTS AND DISCUSSION

2.1 The synthesis of para-cresol gentiobioside

The first reaction in the synthesis of para-cresol gentiobioside as shown in the synthetic route in section 1.3 was a Koenigs–Knorr O-glycosylation reaction, which was discussed briefly in section 1.4. This first Koenigs-Knorr glycosylation reaction carried out in this project involved reacting acetobromo-α-D-glucose, the glycosyl donor along with para-cresol, the glycosyl acceptor which will then form β-D-Glucopyranoside,4-methylphenyl,2,3,4,6-tetraacetate. The reaction also involved using silver triflate which is a very efficient heavy metal promoter in order to activate the glycosyl bromide starting material.[21] Figure 11 below shows the overall reaction for this first step of the synthesis. As the final target compound in this project, para-cresol gentiobioside essentially has only β-glycosidic bonds, it was necessary to control the stereochemistry at each glycosylation step to only form the β-isomer exclusively. This was why the starting material acetobromo-α-D-glucose was chosen as the glycosyl acceptor in this reaction. The presence of the four O-Acetyl protecting groups on the molecule not only blocks those four sites from taking part in the reaction but also aids in stereoselective synthesis of the β-isomer through neighbouring group participation.

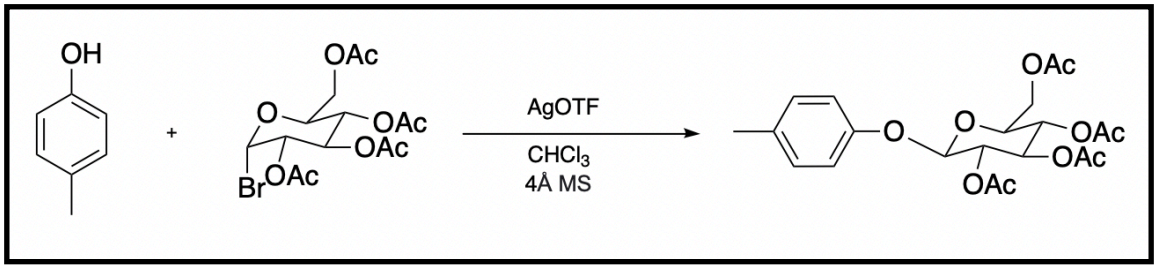

Figure 11 - Overall reaction for step I of the synthesis

In total, three trials for this reaction were performed. The very first trial of this reaction involved stirring a mixture of para-cresol, acetobromo-α-D-glucose, and activated molecular sieves in $CHCl_3$ at 0°C under nitrogen for about 10 minutes. This was then followed by introducing silver triflate into the reaction mixture at 0°C and letting the reaction mixture stir for an additional 2 hours in the dark. After the 2 hour time period, the reaction mixture was then quenched using Et_3N, diluted with $CHCl_3$ and finally filtered through Celite. In the next step the reaction mixture was then purified by an initial separation between $CHCl_3$ and water, followed by a further purification of the organic residue by flash chromatography. The resulting product was then analysed using ^1H NMR spectroscopy. Although the results from the ^1H NMR analysis had revealed that the desired product had indeed been formed, the % yield of the product formed in the reaction was considered to be too low, with only 1.04 grams of the product at a yield of 21% being formed.

Therefore in an attempt to optimise the reaction, it was then decided to carry out another trial of the same reaction. Trial two of the reaction was carried out in the exact same way as in trial one with the only difference being the total reaction time. In this trial instead of stirring the reaction mixture for only 2 hours in the dark, the reaction mixture was allowed to stir for an additional 2 more hours which was about 4 hours in the dark in total. The results from the ^{1}H NMR analysis and the mass of the product isolated had shown a huge increase in the % yield of the product formed in this reaction. In this trial of the reaction, 0.158 grams of the final product at a yield of 35% was properly isolated. Although, in this trial of the reaction, there was an improvement in the % yield of the reaction from 21% to 35%, this was still considered to be unsatisfactory and hence needed further optimisation. An important observation in this reaction was that in addition to being light-sensitive, this reaction was also very sensitive to moisture. This is because in the presence of moisture, water molecules will be able to act as a nucleophile and attack the activated anomeric centre in the original glycosyl donor essentially reforming the starting material glucose, therefore it is necessary that the reaction be performed under extremely dry conditions. It was then understood that the reason for the unsatisfactory % yields in trials one and two were mainly due to the improper activation of the 4Å molecular sieves which acted as the drying agent in the reaction.

In trials one and two of this reaction, the 4Å molecular sieves used in the reaction were activated by heating the sieves in an oven at 80°C overnight prior to the day the reaction was carried out. This was not considered to be sufficient enough to properly activate the molecular sieves. Therefore in order to further improve this step, it was then decided to perform one more trial of this experiment. This third and final trial of the experiment was carried out it in the exact same conditions as in trial two with the only exception which was having the 4Å molecular sieves activated in a different way. The molecular sieves used in this trial were first left to try in an oven at 80°C overnight, which was then followed by setting the sieves on a high vacuum and heating blasting it for a period of 45 minutes with the help of a heat gun. Once again the results from the ^{1}H NMR analysis had shown that desired product had successfully been formed as all the expected peaks corresponding to the different hydrogen environments on the molecule were present on the ^{1}H NMR spectrum. When the final product collected was then weighed, it was found that the % yield in this trial of the reaction was much higher that of both previous trials carried out. In this third and final trial of the reaction, 1.29 grams of the final product at a yield of 53% was successfully prepared. Figures 12 and 13 on the next page show the ^{1}H NMR and ^{13}C NMR spectrums of the final product formed in this reaction.

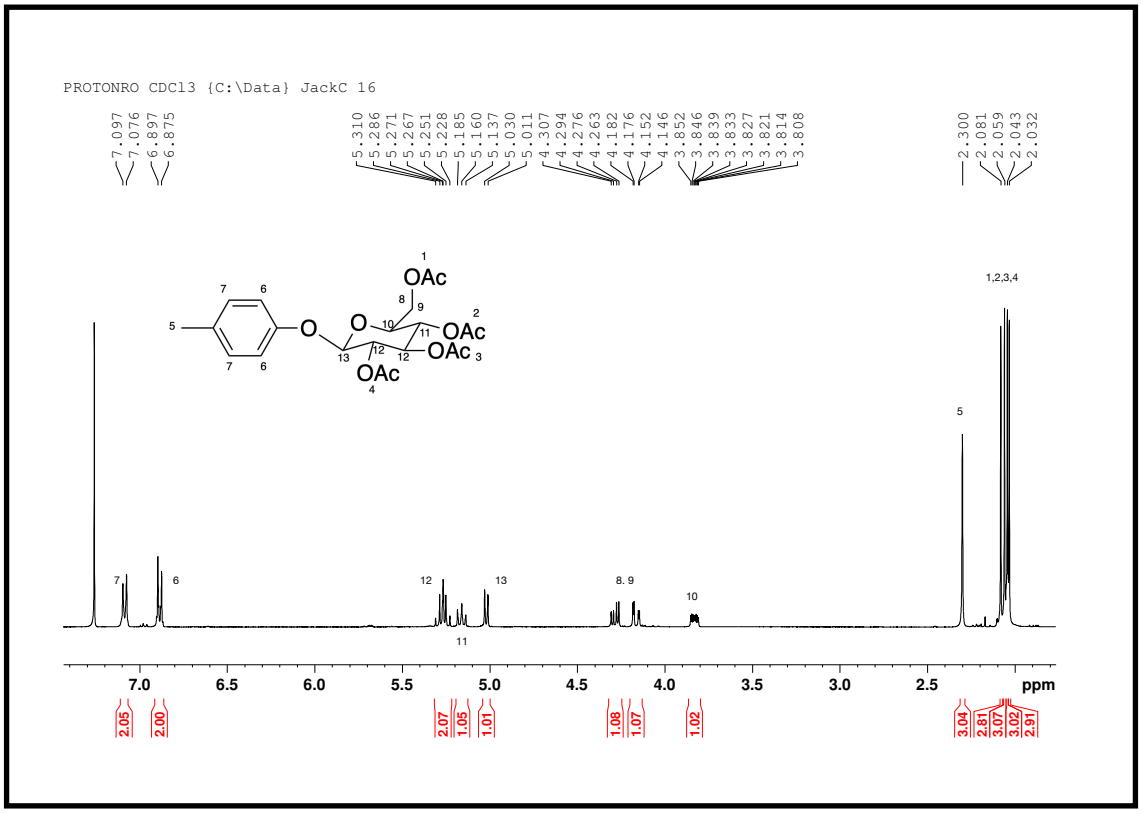

Figure 12 - ^{1}H NMR spectrum of the product formed in step I

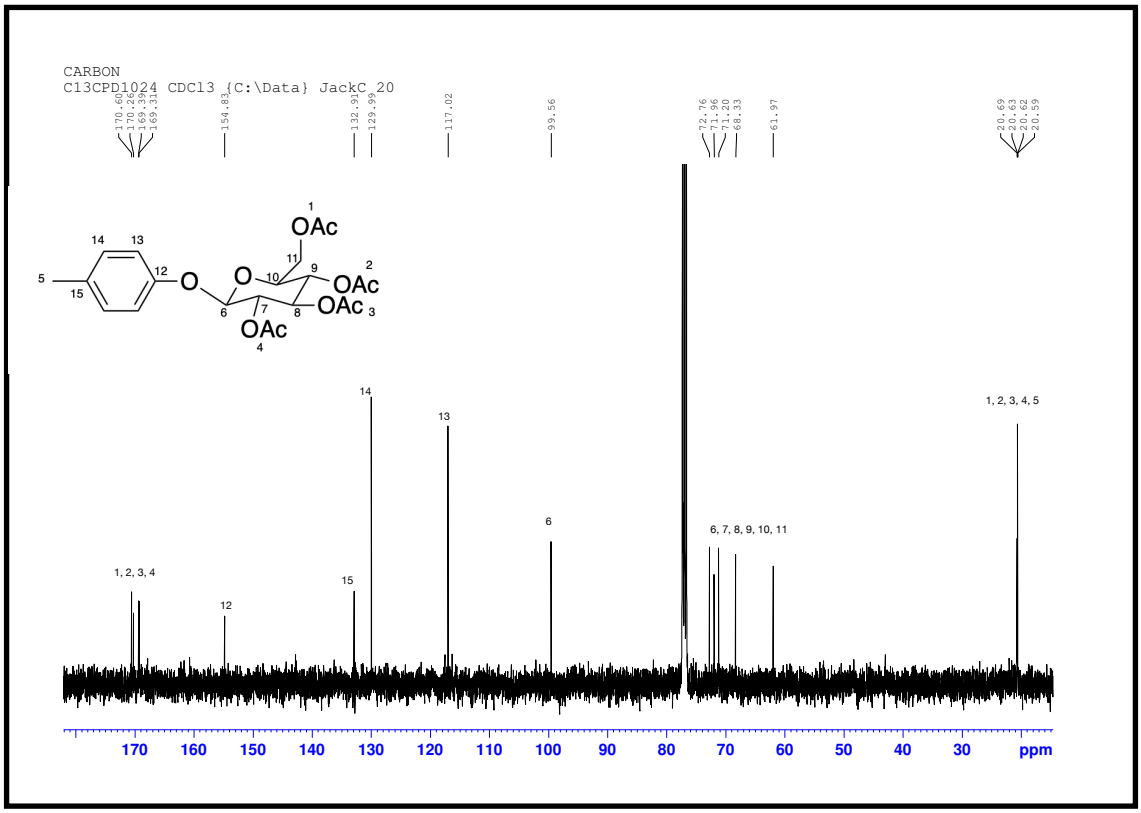

Figure 13 - ^{13}C NMR spectrum of the product formed in step I

The peaks in the ^{1}H NMR spectrum shown in figure 12 corresponding to the different hydrogen environments in the molecule along with the structure of the final molecule shown on the same figure were then used to assign the different peaks. To begin, the four singlet peaks at about 2.00 ppm were easily understood to be that of the 12 protons from the O-Acetyl protecting groups (proton environments 1, 2, 3, and 4). This is because all four peaks in that region had shown to have both the correct multiplicity (singlet, due to no neighbouring protons) and the correct integrations (three protons in each O-acetyl group). To add onto that, it is also well known that a chemical shift of around 2.00 ppm is characteristic for such O-acetyl protecting group protons. Moving on, the singlet peak at 2.30 ppm was then easily assigned to be that of proton environment 5 on the aromatic ring. This is because this was of the right multiplicity (no neighbouring protons) and was also slightly downfield, which was expected due to this group being right next to an aromatic ring which has a deshielding effect. Next, the two aromatic signals seen at around 6.90 and 7.10 ppm were then assigned to be that of proton environments 6 and 7 respectively. This slight difference in the chemical shifts of the two protons environments were due to the presence of the strong electron donating group on the aromatic ring. Such electron donating groups are able to direct electron density onto the ortho-, para- positions due to resonance, which will in turn have a shielding effect on protons in such positions. When it comes to the six signals seen in the range of 3.81 to 5.31 ppm, these were all understood to be from the seven protons from the glucose molecule. The COSY NMR and the HSQC NMR spectra shown in figures 12A and 13A respectively, were then used to assign these protons. As the HSQC spectrum show the peaks at 4.15 and 4.28 ppm to be of a different phase, this immediately suggests that they must be from each proton of the $-CH_2$ group in the glucose molecule (proton environments 8 and 9). From the COSY spectrum it is then possible to see that the only neighbouring proton signal to this $-CH_2$ group is the signal at 3.82 ppm, which was then assigned as proton 10. Moving on, the COSY spectrum also shows that the proton signal 10 is close to the triplet signal at 5.16 ppm which was then assigned as proton 11. As proton 11 on the spectrum is then close to the multiplet at 5.30 ppm, this means this signal must be due to proton environment 12. The only remaining signal, the doublet peak at 5.02 ppm was then identified to be that of the proton on the anomeric carbon. Once all the ^{1}H NMR signals have been assigned, the signals on the ^{13}C NMR corresponding to those different environments can be assigned relatively easily using the HSQC NMR. Additionally it is worth mentioning that the carbon signal at around 100 ppm is characteristic of a glycosidic carbon and was a good indicator that the glycoside had been successfully formed in this reaction.

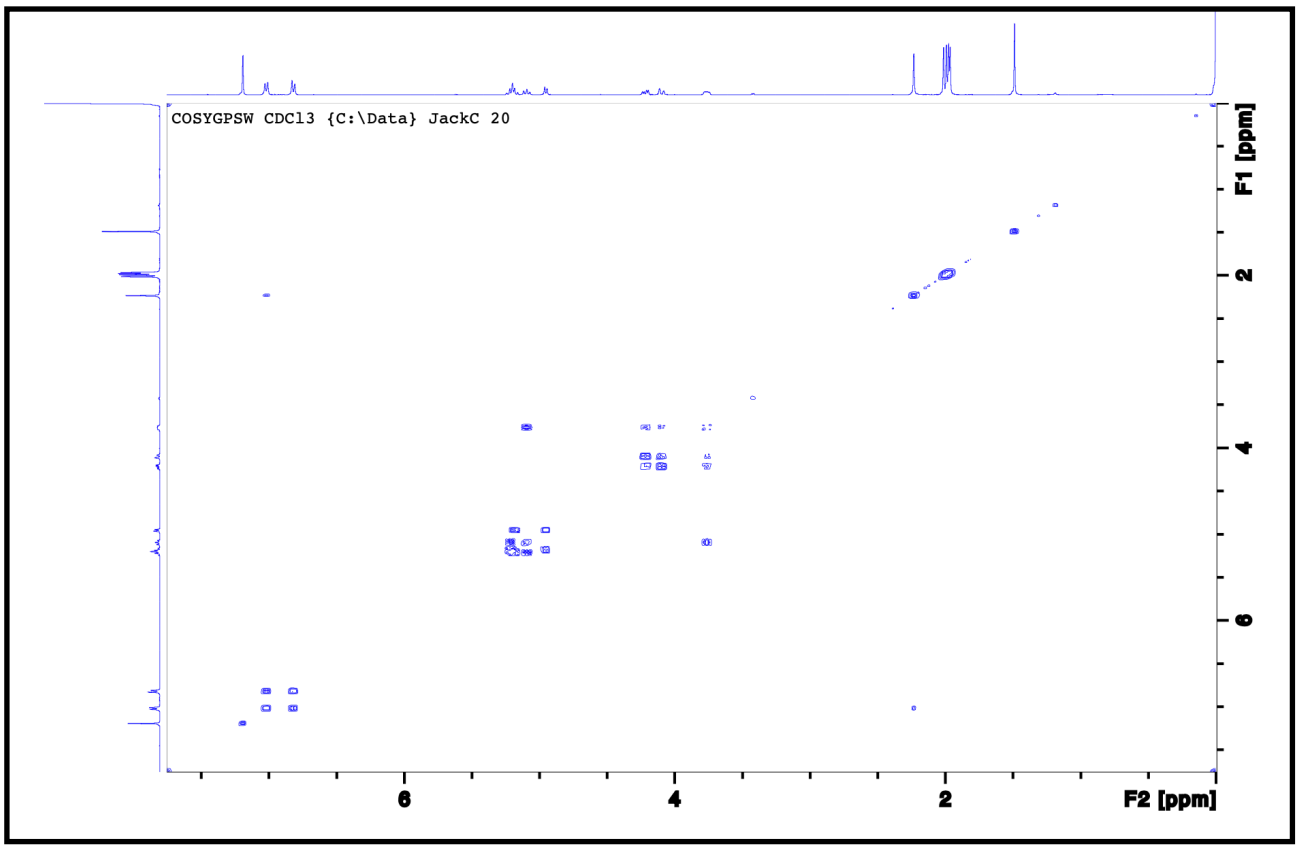

Figure 12A - COSY NMR spectrum of the product formed in step I

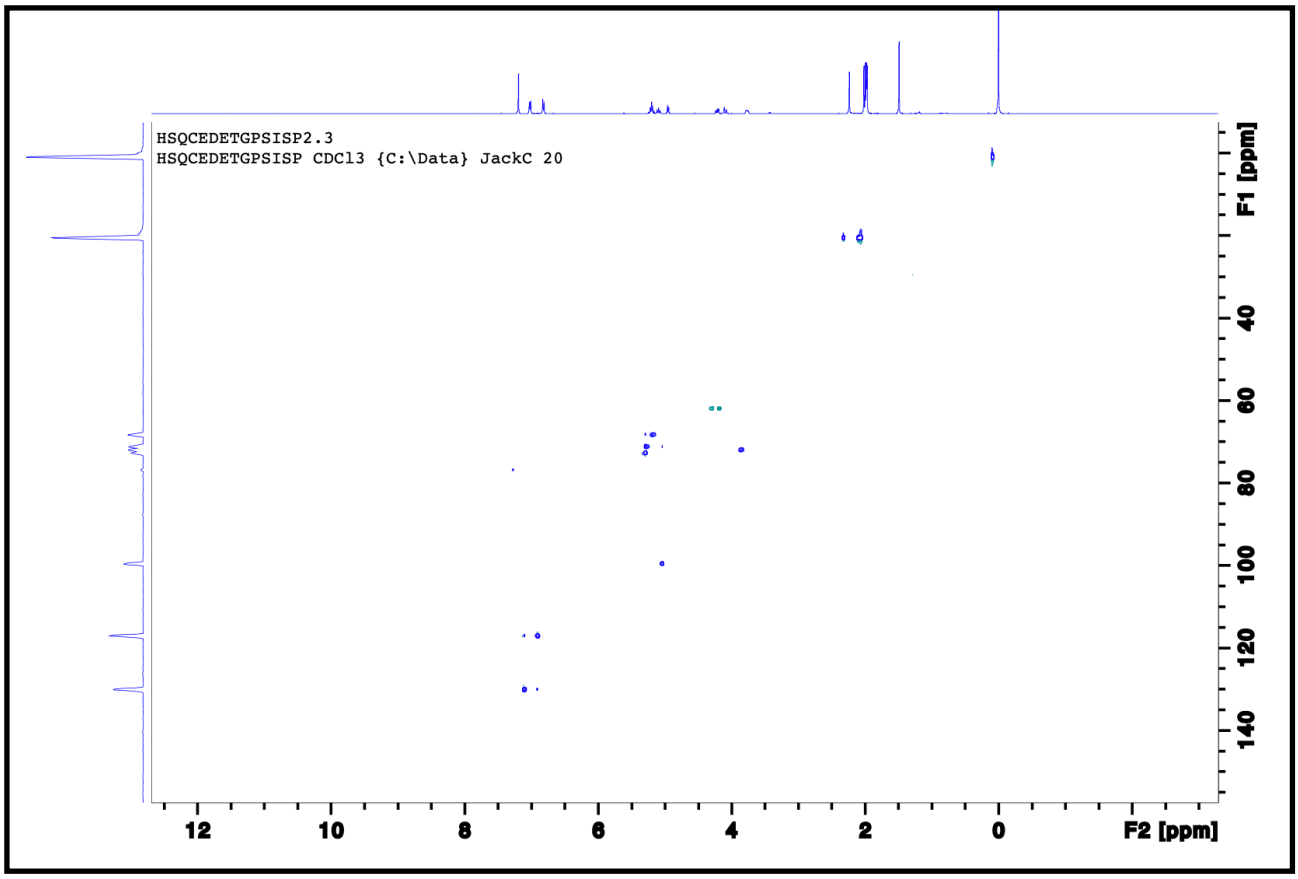

Figure 13A - HSQC NMR spectrum of the product formed in step I

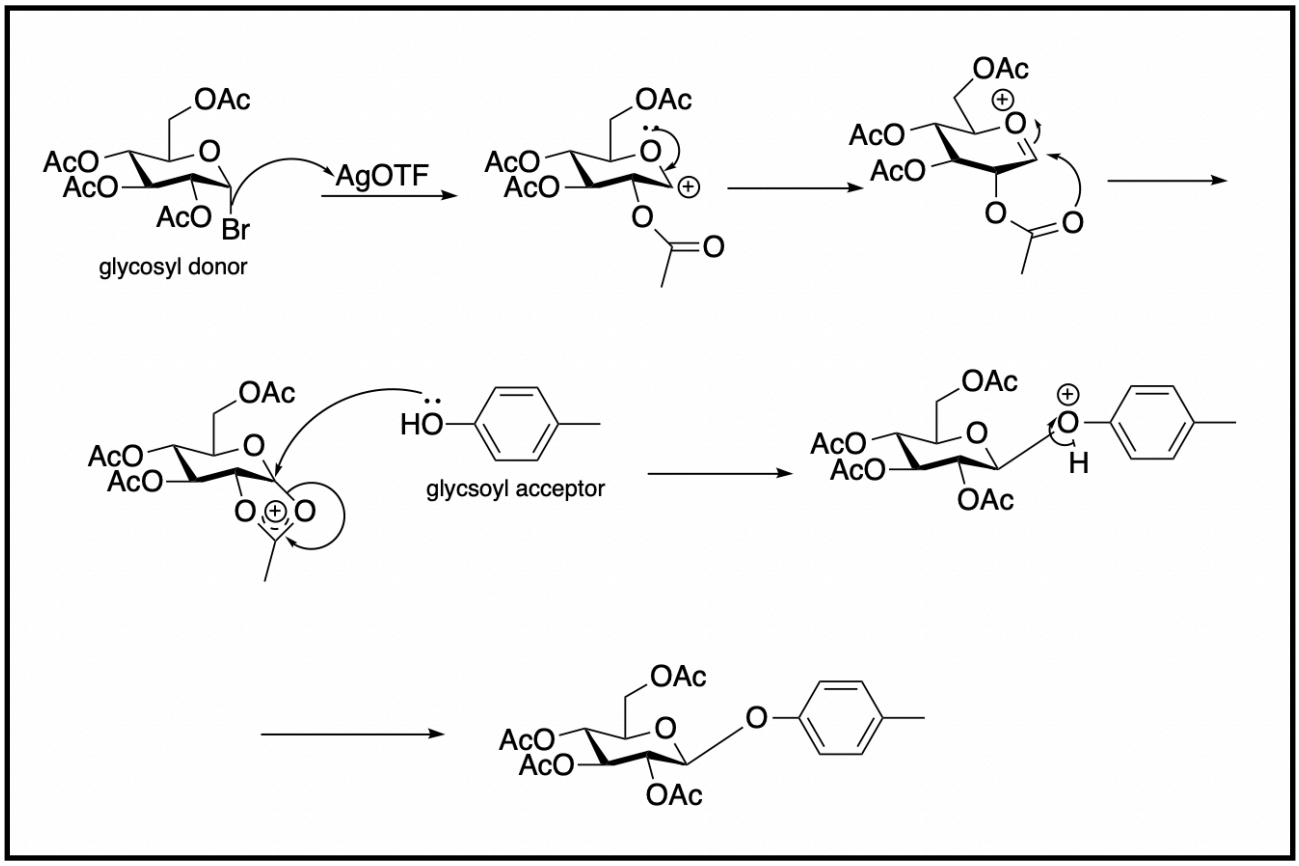

Figure 14 - The reaction mechanism for step I of the synthesis

Additionally, figure 14 above shows the overall mechanism of this first glycosylation reaction that was carried out. The mechanism starts off with the action of the promoter, AgOTF, which works by aiding in the removal of the bromide ion leaving group from the glycosyl donor, which was acetobromo-α-D-glucose. This is in turn results in the activation of the anomeric carbon in the glucose molecule, which is now in an carbocation state as shown on the diagram. In the next step the movement of electrons from the ring oxygen will now form the oxocarbenium ion as shown in the diagram. In normal circumstances, the glycosyl acceptor which is para-creosol will be able to attack the anomeric carbon from both the upper and lower faces which will result in the formation of both the α- and β-anomers. However in this case, due to the acetobromo-α-D-glucose molecule having a neighbouring group active protecting group (the O-acetyl group) at the C-2 carbon, there will be movement of electrons from the carbonyl oxygen onto the anomeric carbon. What this effectively does it that it now completely blocks one face (the bottom face) of the anomeric carbon and will only allow the glycosyl acceptor to attack the anomeric carbon from the upper face. Therefore as a result of this, the compound formed in this step will exclusively be the β-anomer.

Additionally, it was important to mention that another optimisation reaction was carried out for this first glycosylation step in this project. This was carried out according to what was stated in the literature.[30] It was found that the % yield for the product formed in this reaction turned out to be even higher than that of the previous reaction which used silver triflate as the promoter. This reaction involved having a slightly different glycosyl donor which was penta-O-acetyl-β-D-gluco-pyranose, reacting with para-cresol which was the glycosyl acceptor. Only one trial of this reaction was carried out and it was performed in a similar way to what was reported in the literature. The reaction involved adding a solution of triethylamine in DCM to a mixture of para-cresol and penta-O-acetyl-β-D-gluco-pyranose under nitrogen. In the next step, a solution of $BF_3.OEt_2$ in DCM, which is understood to be the catalyst in the reaction, was then added dropwise to the mixture. After letting the mixture stir for a period of 24 hours, the reaction mixture was then quenched with sat. $NaHCO_3$. After an initial separation with EtOAc, the organic residue was then further purified by flash chromatography. In the last step, the final product collected was the analysed using ^1H NMR spectroscopy. Once it was confirmed from the ^1H NMR spectrum that the desired product had been formed, the final product was then collected and properly stored. 0.164 grams of the desired product at a yield of 73% was prepared in this reaction. Figure 15 below shows the overall reaction for this additional optimisation reaction. Although this glycosylation reaction had proven to be a much better alternative to the original one carried out previously, it did not make its way into the synthetic scheme for this project as it was performed at a much later stage after the entire synthesis for para-cresol gentiobioside was completed.

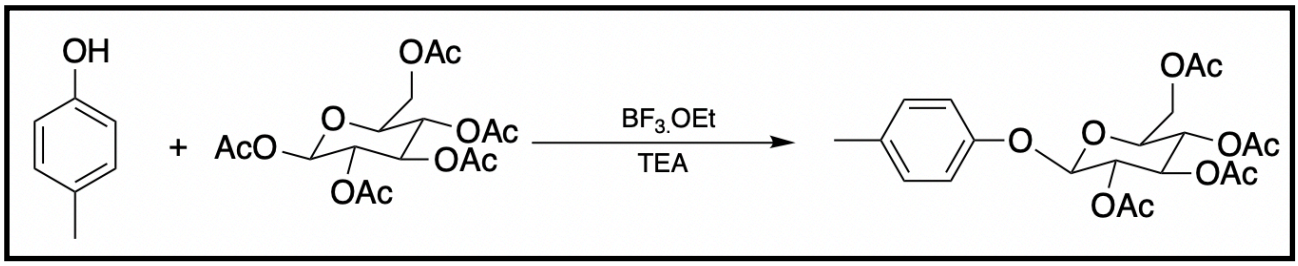

Figure 15 - Overall reaction for the alternative reaction for step I

Once step one in the synthesis was successfully carried out, it was then decided to proceed onto step two of the synthesis. This was performed in the same method that was stated in the literature.[31] Step two in the synthetic scheme for para-cresol was relatively simple to carry out and involved having a global de-protection of all the O-acetyl groups in the molecule. Figure 16 below shows the overall reaction for this step in the synthetic scheme.

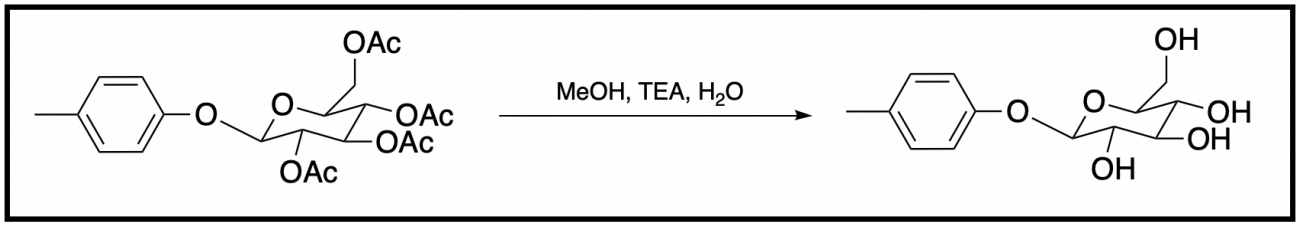

Figure 16 - Overall reaction of step II of the synthesis

Three trials for this reaction was carried out, and all trials were performed in the exact same way. These reactions involved having the product from the previous step being collected and dissolved in a mixture of MeOH, Et_3N, and H_2O. The reaction mixture was then left to stir for a period of 24 hours. On completion of the 24 hour time period, the reaction mixture was repeatedly evaporated with water under reduced pressure in order to remove triethylamine. This was carried out until there was no further change in the mass of the solid residue. In the final step, the final organic residue was then analysed using ^{1}H NMR spectroscopy and ^{13}C NMR spectroscopy, to find that the final compound was present. The most successful run in this reaction saw 0.779 grams of product at a yield of 98% be synthesised. An interesting observation was that the compound prepared in this step was no longer soluble in deuterated chloroform, which was used as the NMR solvent in the previous solvent, and had to be dissolved in deuterated methanol instead. This was expected as the product formed in this step was much more polar than that of the previous step due to it having four highly polar -OH groups in the molecule. Figures 17 and 18 on the next page show the ^{1}H NMR and ^{13}C NMR spectrums for the intermediate prepared in this step of the synthetic scheme. From the ^{1}H NMR spectrum shown on figure 17, it is possible to see that the only signals present are those from the aromatic ring (signals at 7.00 and 6.90 ppm), glucose component (signals from 3.23 to 3.82 ppm which integrate for the 7 protons present in the glucose component) and the methyl group on the aromatic ring (signal at 2.19 ppm). This alone confirms that the desired product was present, as all proton signals from the four O-acetyl groups, that was seen in the ^{1}H NMR spectrum for step one, are no longer present on the spectrum (since these groups were de-protected). This can also be seen on the ^{13}C NMR spectrum with the peaks due to the carbonyl carbons at around 170.0 ppm not being present anymore.

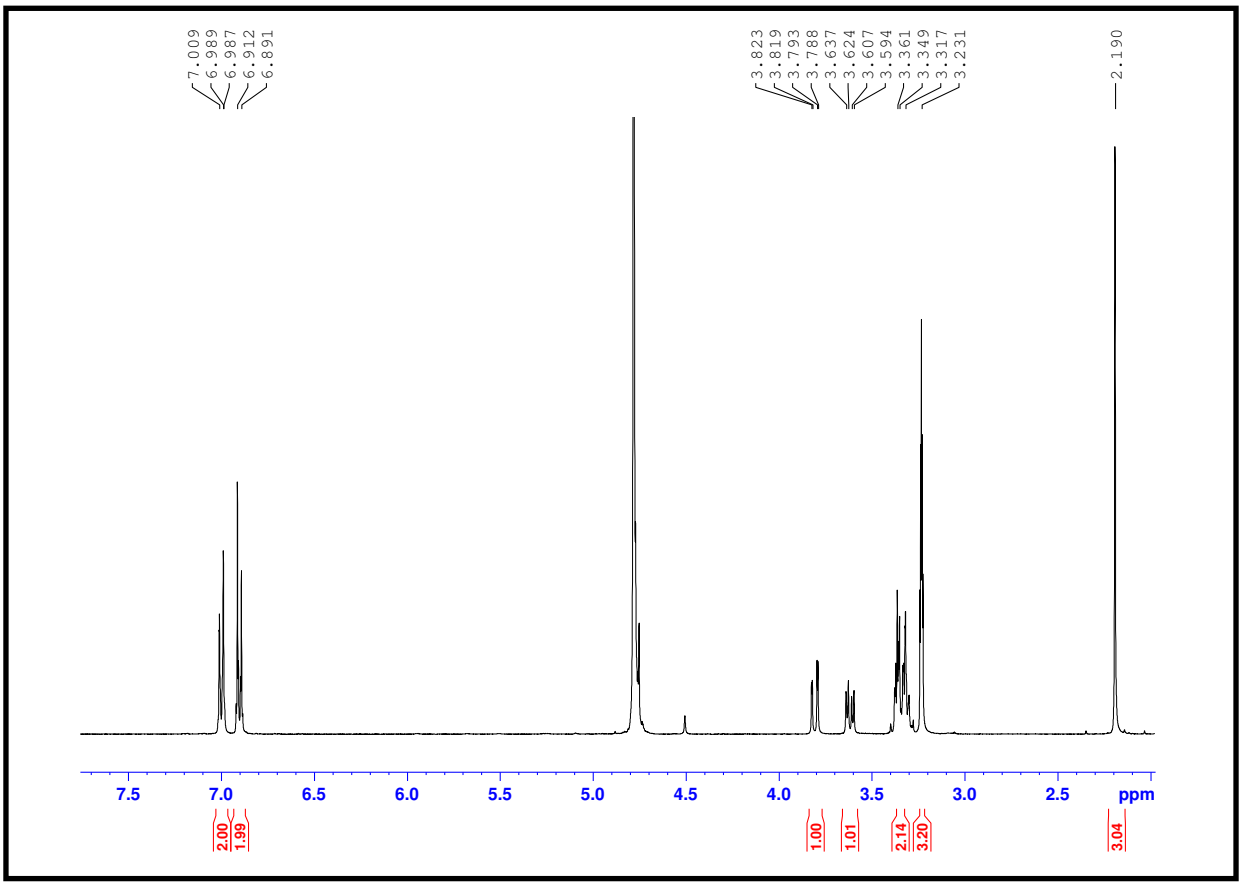

Figure 17 - ^{1}H NMR spectrum of the product formed in step II

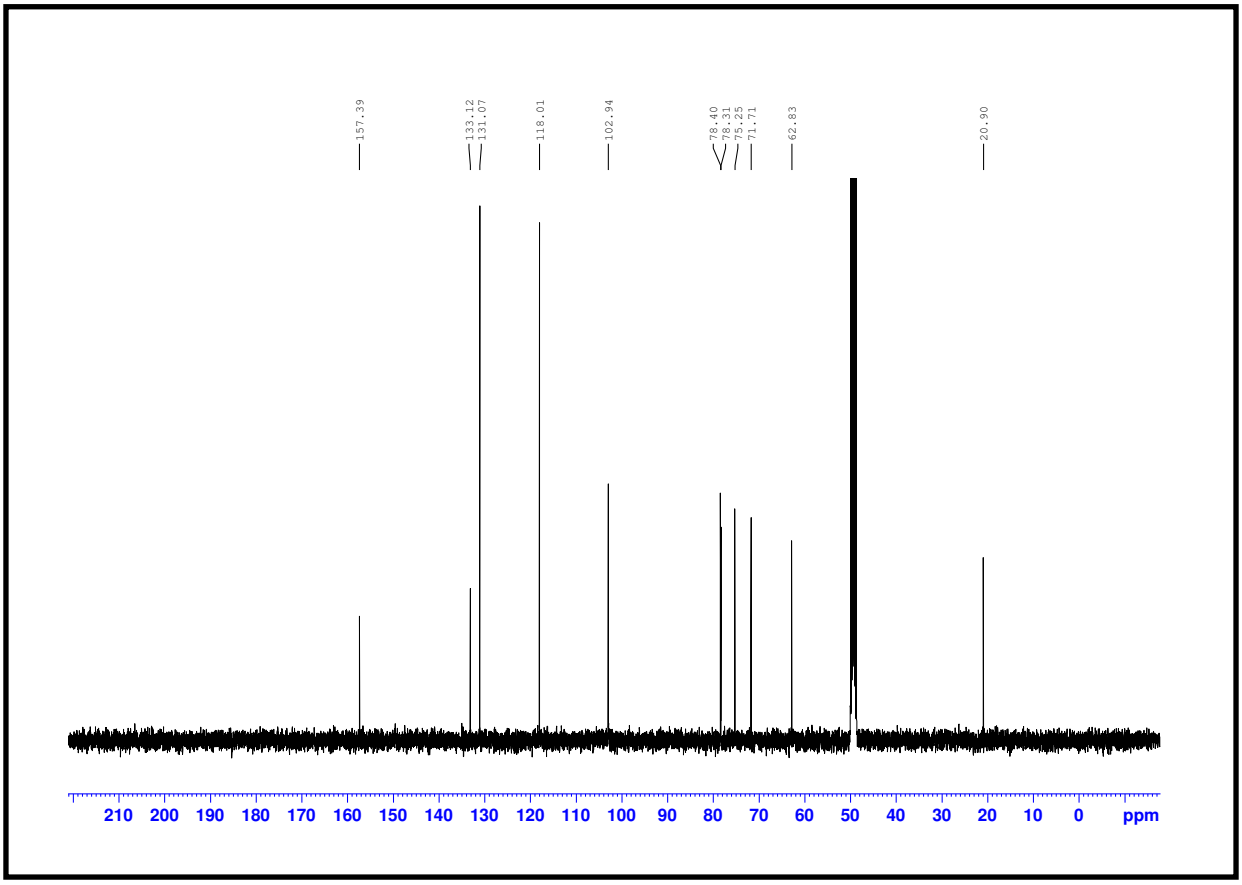

Figure 18 - ^{13}C NMR spectrum of the product formed in step II

After step two of the synthesis was completed, all product from that step was carried over to the next reaction in the synthetic scheme. This step in the project was actually a selective protection of the primary -OH group on the C-6 carbon atom. Figure 19 below shows the overall reaction for this step of the project.

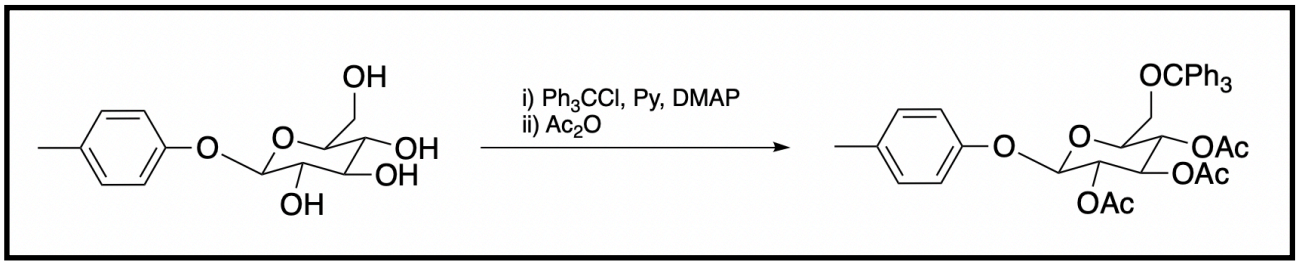

Figure 19 - Overall reaction for step III of the synthesis

As the final molecule in the project, para-cresol, also had a second glycosidic linkage at the C-6 carbon atom, there needed to be a way to ensure that only the primary -OH group on the C-6 carbon atom acts as the glycosyl acceptor and all the other -OH groups do not react. This was why the reactions in step three (the current one) and step four were introduced into the synthetic scheme in this project. To explain, steps three and four were a protection and de-protection strategy that utilised the different reactivities of the -OH groups in the sugar in such a way that only the primary -OH group on the C-6 carbon atom remains de-protected while every other -OH group on the molecule will be acetylated (protected). In general, the reactivity order in sugars is primary -OH > equatorial -OH > axial -OH, which is mainly due to steric factors.[32] Therefore with the help of a bulky reagent such as triphenylmethylchloride[32], which was used in the current step, a very high yield of the 6-O-monoprotected compound can be obtained. Next, with the help of an acetylating reagent such as acetic anhydride all remaining -OH groups can be protected. Once this is complete, the fully protected molecule will now have two types of orthogonal protecting groups which can now be selectively removed independent of each other. This is exactly what is done step four of this project, which will be seen shortly.

Returning back to step three of the project, two trials of this reaction were performed. The first trial of this reaction involved carefully adding anhydrous pyridine to a mixture of the product from the previous step, DMAP, and triphenylmethylchloride under nitrogen. The reaction was carefully monitored by TLC whilst stirring at 60°C for a period of 6 hours. On completion of the 6 hour time period, analysis by TLC had shown a new spot which was much more non-polar than that of the starting material, this was understood be that of the 6-O-monoprotected product. At this point, acetic anhydride was then added in order to acetylate all remaining -OH groups, and the reaction was left to stir for an additional 3 hours. On completion of the reaction, the reaction vessel was placed on ice, which was then followed by an addition of methanol and then letting the mixture to stir for an additional 30 minutes. In the next step after removing the solvent under reduced pressure, an extraction was carried out using DCM and water. In the final step, the collect organic residue was then purified by flash chromatography.

When the pure organic compound collected was analysed using ^{1}H NMR spectroscopy, it was found that the pure product had successfully been isolated. 0.314 grams of the desired product at a yield of 76% was collected from this first trial. Although this trial of the reaction did produce pure product, the % yield of the reaction, which was 76% was not considered to be satisfactory at the time and hence another trial of the reaction was carried out. When the previous trial was carried out, the results from the TLC analysis had shown that a time period of 6 hours for the first half of the reaction was unnecessary as the reaction had clearly gone to completion at the 4 hour time mark. To add onto that it was also observed that the second half of the reaction, which saw the acetylation of all remaining -OH groups, did not go to completion even after the 3 hour time period. Therefore in an attempt to further optimise the reaction, a second trial was carried out with a few minor changes. These minor changes included stirring the reaction mixture in the first part only for a period of 4 hours at 60°C and then instead of stirring the reaction mixture in the second part for a period of 3 hours, the reaction mixture was let to react overnight. When the pure compound post purification was weighed, it was found that the % yield of this trial was much higher than that of the previous trial. 1.22 grams of the pure product was prepared in this trial at a yield of 86%. Figure 20 shown below shows the ^{1}H NMR spectrum of the final organic residue from this trial of the reaction.

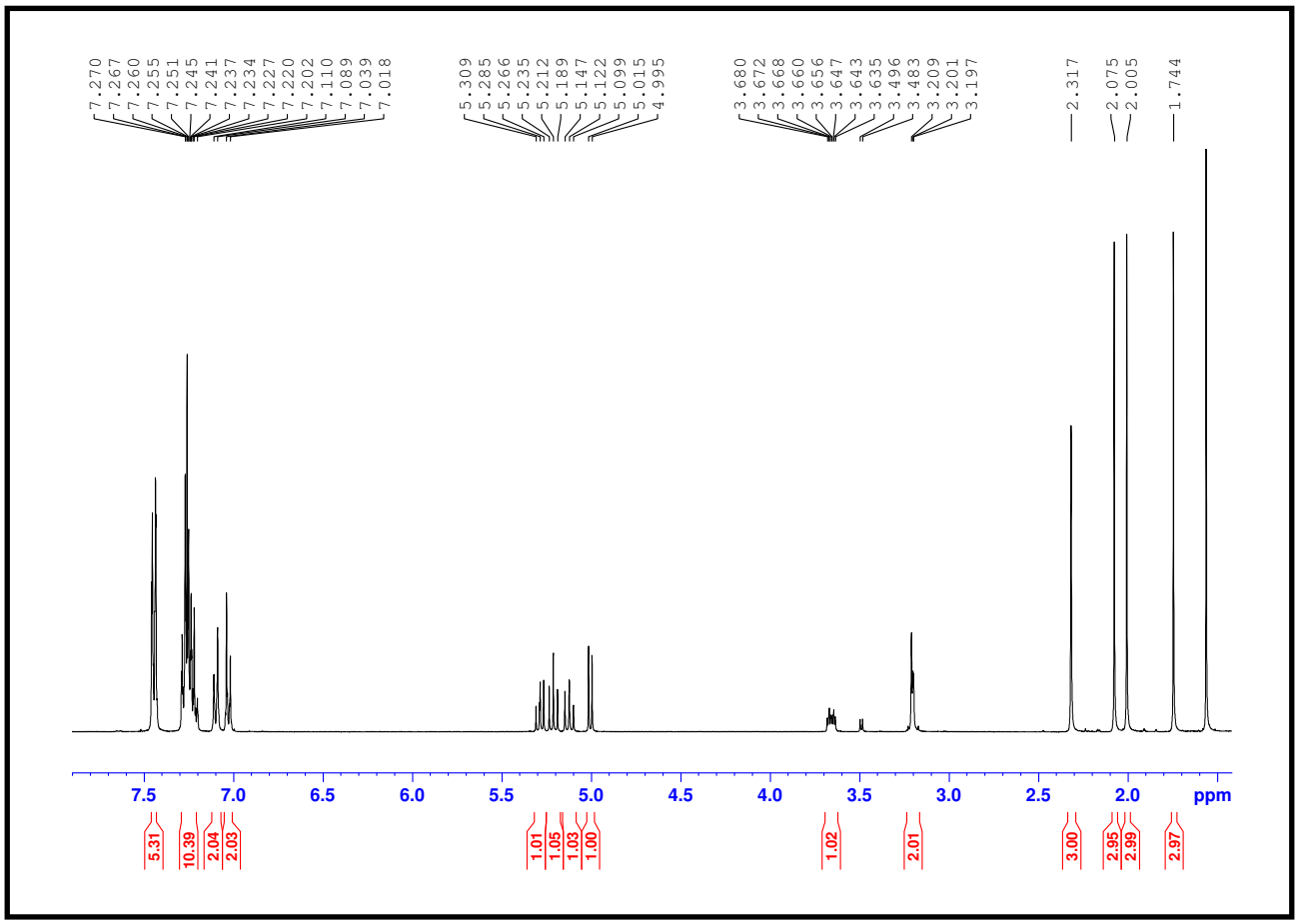

Figure 20 - 1H NMR spectrum of the product from step III

From the ^{1}H NMR spectrum shown on the previous page, due to having assigned most of these peaks previously, it was relatively easy to identify all signals due to the glucose component (range 3.20 to 5.31 ppm), aromatic ring (two doublet signals at 7.02 and 7.10 ppm), and the methyl substituent on the aromatic ring (peak at 2.32 ppm). It is also possible to see a few new peaks, which were three singlet peaks at around 1.74, 2.01, and 2.08. These three singlet peaks correspond to the protons from the three O-acetyl protecting groups that were introduced into the molecule in this step. Moving on, in addition to the two aromatic signals from the original para-cresol component, a few other aromatic signals were observed. These additional signals were all from the bulky trityl protecting group that was introduced into the molecule in this step. The total integrations of these additional aromatic peaks all add unto 15 protons, which is exactly the number of protons present in one trityl protecting group.

As step three in the synthesis was now complete, it was time to move onto the next step of the synthesis. This step as mentioned previously will be a selective de-protection reaction of only the triphenylmethyl (trityl) protecting group on the C-6 carbon atom. Such trityl protecting groups are generally considered to be stable under basic conditions but they can be selectively removed in the presence of a mild acid such as acetic acid, which is exactly what is done in this step of the project. Figure 21 below shows the overall reaction of this de-protection step.

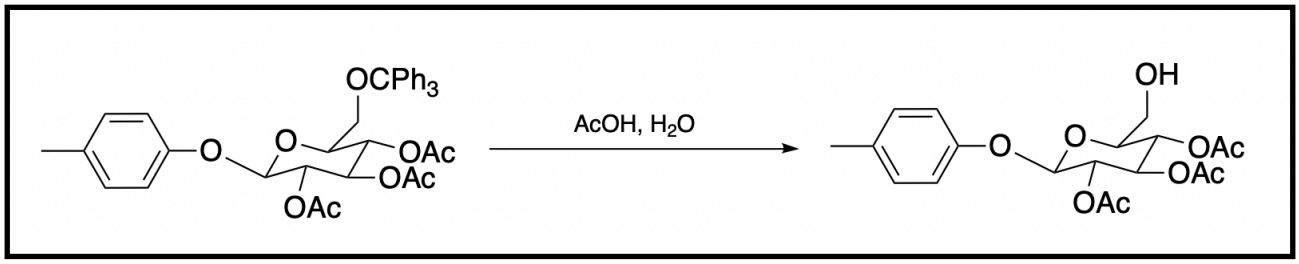

Figure 21 - Overall reaction for step IV in the synthesis

In total two trials were carried out for this step in the project. The first trial performed involved dissolving the product from the previous step in a mixture of acetic acid and water. The reaction mixture was then left to heat under a reflux at 100°C for a period of 1 hour. After the 1 hour time period, the heating was stopped and the reaction mixture was then left to stir at room temperature overnight. In the next step, the resulting crystals were then filtered and washed with 75% methanol, which was then followed by an evaporation of the solvent under reduced pressure. To end, the final organic residue was then purified by flash chromatography. The results from the 1H NMR analysis along with the mass of the product collected had shown that the desired product was successfully recovered. In this first trial, 0.300 grams of pure product at a yield of 43% was collected.

When the first trial of the reaction was carried out, one observation from the TLC analysis was that the reaction had not completely gone to completion. Therefore in trial two of the reaction, in order to get a better yield of the product a slight change was made to the procedure carried out. This change involved heating the reaction mixture under reflux for a period for 2 hours instead of the original 1 hour time period. It was later found that this slight change that was made had a positive impact on the overall yield of the reaction, as 0.290 grams of the product at a yield of 54% was recovered. Figure 22 below shows the ^{1}H NMR spectrum from the ^{1}H NMR analysis of the final pure product from this step. Once again due to previously assigning most of these signals, it is easy to see the signals from the original aromatic component (two doublets at 6.87 and 7.10 ppm), seven protons from the glucose component (range 3.61 to 5.35 ppm), and also the methyl substituent on the aromatic ring (singlet at 2.30 ppm). Additionally it was also easy to spot the three singlets that correspond to the protons from the three O-acetyl protecting groups in the molecule. These three signals were at 2.04, 2.05, and 2.07 ppm. One good indicator that the reaction had produced the desired product was that in this spectrum all additional aromatic signals (due to the trityl protecting group) were no longer present.

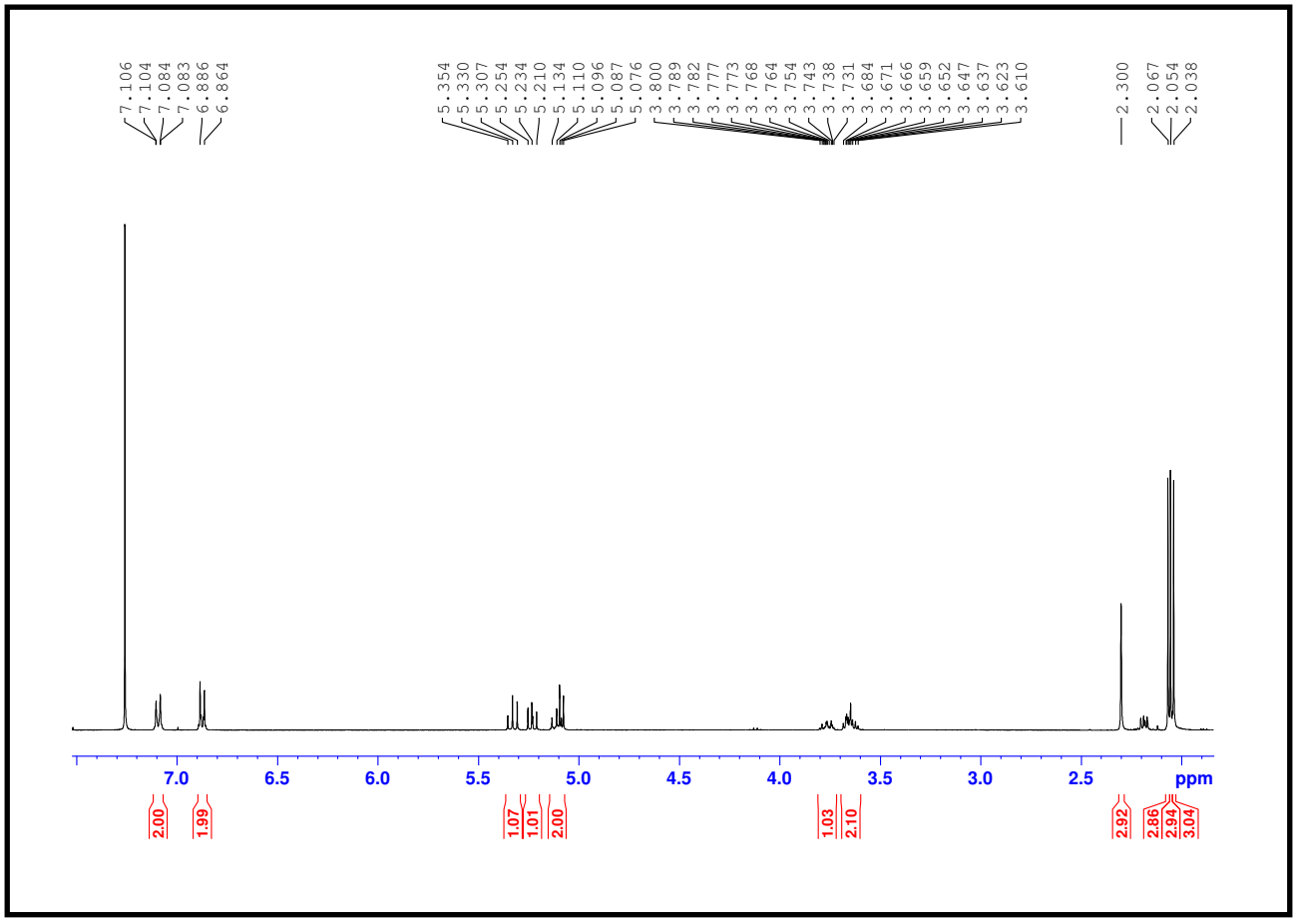

Figure 22 - 1H NMR spectrum of the product from step IV

Once step four of the project had been completed, it was then decided to proceed onto the next step. Step five in the synthetic scheme for para-cresol was a key reaction and was another Koenigs–Knorr O-glycosylation reaction which will see the formation of the second glycosidic linkage in the molecule. The main difference in this glycosylation reaction, as opposed to the first one in the synthesis, is that the free -OH group on the C-6 carbon atom will now be acting as the glycosyl acceptor which will react with acetobromo-α-D-glucose, the glycosyl donor. The main similarity however, is that the product formed in this step will once be the β-anomer exclusively. This due to the neighbouring group participation of the O-acetyl group on the C-2 carbon atom of the acetobromo-α-D-glucose molecule. In total, three trials were carried out for this reaction. The very first trial of this O-glycosylation reaction was carried out using a milder promoter in the form of Ag_2O, which was very similar to the method as stated in the literature.[31] Figure 23 below shows the overall expected reaction for this first trial carried out.

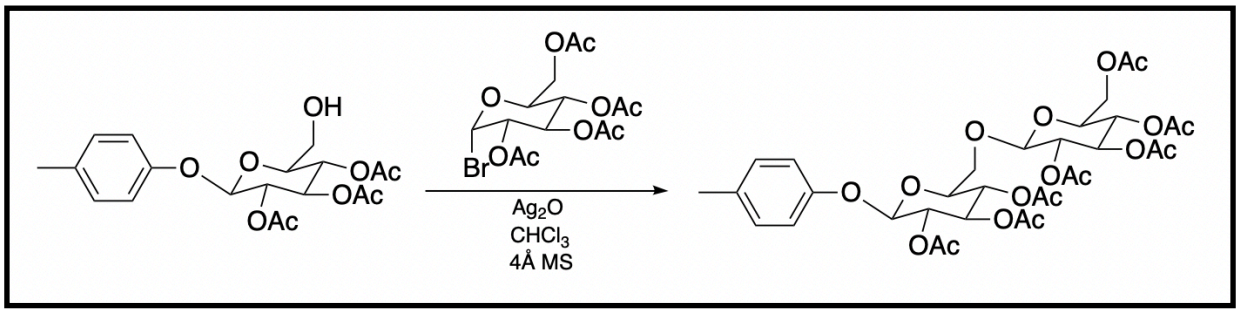

Figure 23 - Overall reaction of the alternative reaction done for step V

This trial involved first preparing a solution of acetobromo-α-D-glucose in $CHCl_3$. This prepared solution was then added dropwise in the darkness to a stirred solution of the product from the previous step, Ag_2O, and activated 4Å molecular sieves in $CHCl_3$. It is important to mention that the molecular sieves used in all experiments here were activated using the same optimised method that was performed earlier in step one of the synthesis. The reaction mixture, after adding all reagents, was then stirred at room temperature for a period of 30 minutes. This was then followed by a filtration of the reaction mixture, and then a removal of solvent under reduced pressure. In the final step, the remaining organic residue was then purified by flash chromatography and then analysed using ^1H NMR spectroscopy. As the results from the ^1H NMR analysis had shown no conclusive evidence of the desired product being present, this trial of the reaction was ruled out as a potential method.

As the method using Ag_2O as a promoter clearly did not work, another trial of the reaction was then carried out. This trial of the reaction was carried out in the exact same way as the previous one, with the only change being the usage of silver triflate as a promoter instead of Ag_2O. Figure 24 on the next page shows the overall reaction for this trial of the reaction.

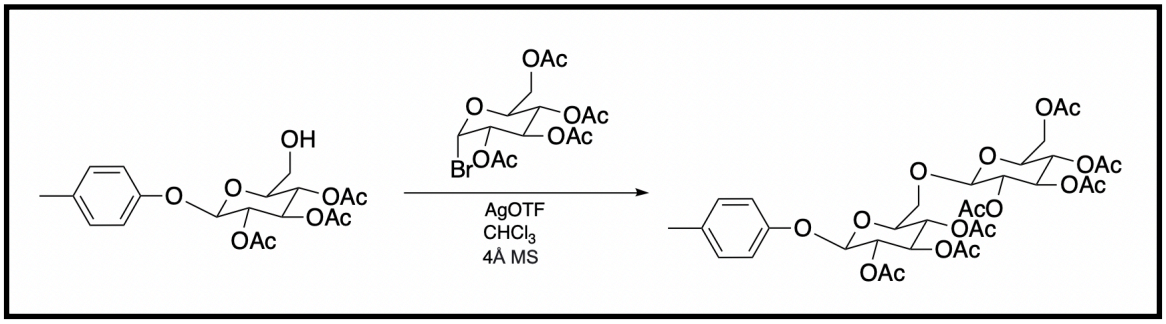

Figure 24 - Overall reaction for step V of the synthesis

This change was made as it was already known that the silver triflate worked very well when used in the first step of the synthesis. On completion of the 30 minute time period, the reaction mixture was then filtered and evaporated under reduced pressure. The purified organic residue post flash chromatography was then analysed using ^{1}H NMR spectroscopy. Although it was identified from the ^{1}H NMR spectrum that the desired product was present, the major issue was that the organic residue collected was still impure and was essentially a mixture of both the starting material and the product. At this point it was understood that both the starting material (the product from the previous step) and the product in this step had the same R_f value and therefore could not be separated via flash chromatography alone. From previously knowing that the starting material was soluble in methanol and the product was not, the pure product in this step was isolated as a precipitate using the preferential solubility of the starting material in methanol. Once the purity of the compound had been confirmed by another ^{1}H NMR analysis, the resulting product was then collected and weighed. 0.0420 grams of the pure compound at a yield of 20% was recovered from this step of the reaction. Although the reaction in this trial had yielded a positive result, the % yield of the reaction was considered to be too low at the time and had to be improved slightly. This was when it was decided to perform another trial of the reaction. This third and final trial of the reaction was carried out in the exact same way as the previous trial, where the only difference was that the reaction was now allowed to stir for a period of 4 hours at room temperature instead of 30 minutes. On completion, the reaction mixture was then filtered, and then evaporated under reduced pressure to remove the solvent. After an initial purification by flash chromatography, the resulting organic residue was then further purified by precipitation with methanol. The pure compound, once confirmed by ^{1}H NMR analysis, was then collected and weighed. It was found that the % yield of the reaction in this trial was slightly improved, as 0.154 grams of the desired product at a yield of 29% was properly isolated. Figures 25 and 26 on the next page show the ^{1}H NMR and ^{13}C NMR spectra respectively, of the pure product collected in this step. One good indicator that the reaction had produced the desired product was that now there is total of 14 protons instead of 7 protons in the region from 3.50 to 5.50 ppm. This was expected as the final product in this step includes a disaccharide (two sugar units) and would hence have double the number of protons.

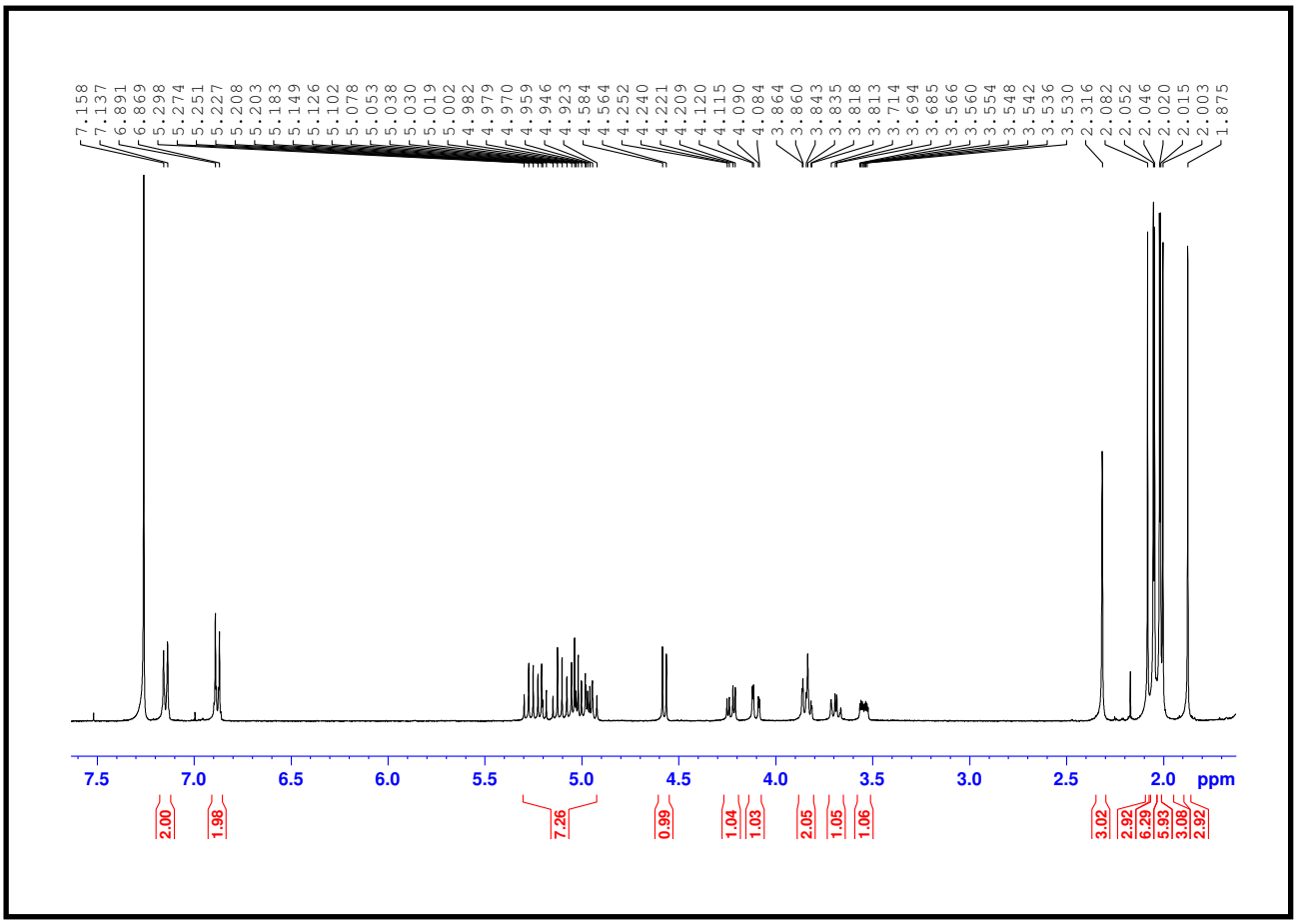

Figure 25 - ^{1}H NMR spectrum of the product from step V

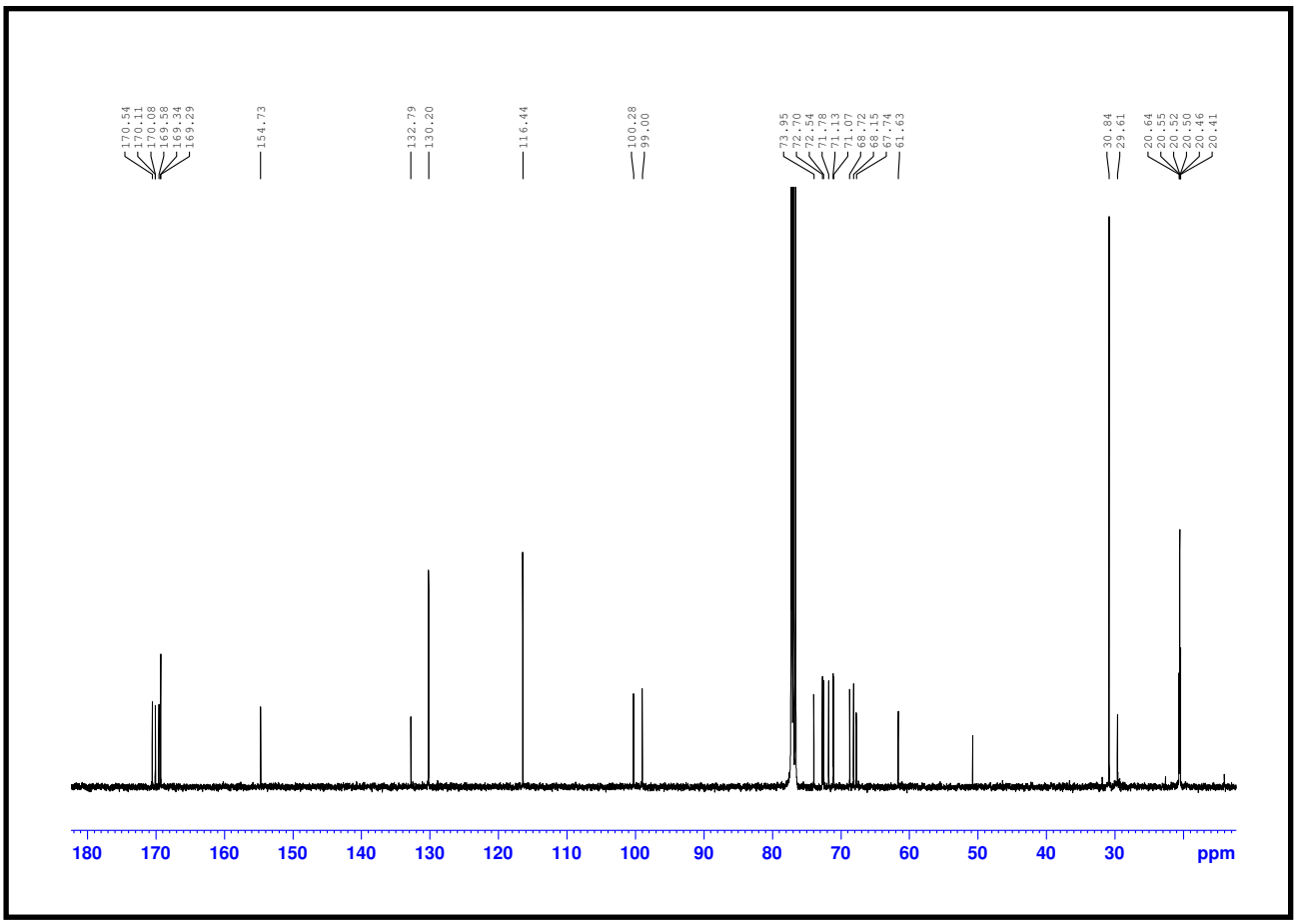

Figure 22 - ^{13}C NMR spectrum of the product from step V

With the completion of step five, it was then decided to proceed onto the last and final step of the synthesis. This step was another global de-protection of all the O-acetyl groups in the molecule to give the final compound in this project, which is para-cresol gentiobioside. This final step in the project was carried out in the exact same way as step two of the project, which was also a global de-protection of all the O-acetyl groups on the molecule. Three trials were carried out for this final reaction in the synthesis, and all trials were carried out in the exact same way. Figure 27 below shows the overall reaction for this final step in the project.

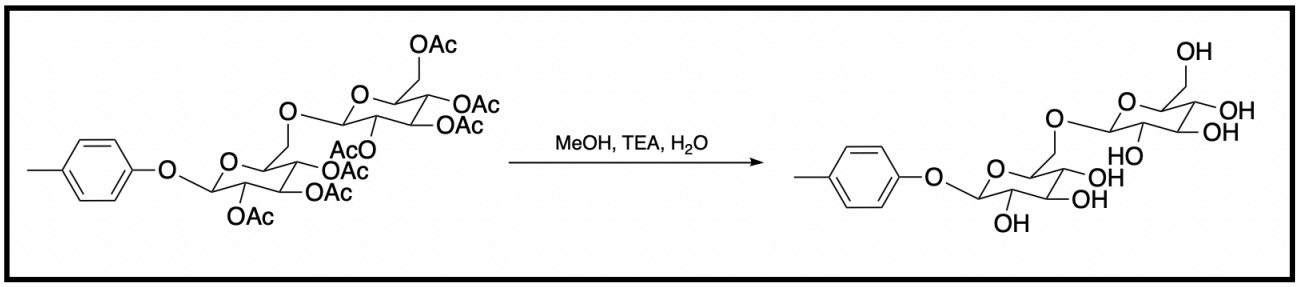

Figure 27 - Overall reaction for step VI in the synthesis

These trials involved dissolving the product from the previous step in a solution of methanol, water, and triethylamine, which was then followed by letting the mixture to stir for a period of 24 hours at room temperature. In the next step the reaction mixture was then repeatedly evaporated with water under reduced pressure until there was no further change in mass. When the resulting organic residue was then analysed using ^{1}H NMR spectroscopy, it was found that the compound collected was not pure and was a mixture of the starting material and product. Once again much similar to the purification performed in step five, the product in this step was isolated as the filtrate using the preferential solubility of the same product in methanol. The best trial of this final reaction saw 0.0750 grams of the final product at a yield of 97% be prepared. Figures 28 and 29 on the next page show the ^{1}H NMR and ^{13}C NMR spectra for the final pure product, the novel compound para-cresol gentiobioside. From the ^{1}H NMR spectrum, one good observation was that the signals due to the presence of the O-acetyl protons are now no longer present. This shows that the de-protection of these O-acetyl groups has properly occurred yielding the final compound in the project, para-cresol. To add on, it was also noticed that the summation of all the integrals in the ^{1}H NMR spectrum all add up to 21 protons which was the exact number of protons present in para-cresol gentiobioside. Additionally, a low resolution mass spectrum and also an IR spectrum were also obtained and these are shown on figures 30 and 31 respectively. From the IR spectrum obtained the broad, high intensity peak at 3232 cm^{-1} was expected as the final compound had multiple -OH groups in its structure. Lastly, the low resolution mass spectrum obtained gave hard evidence as the $[M+Na]^{+}$ peak (molecular ion peak) was a match with the molar mass of the final compound plus that of the sodium ion.

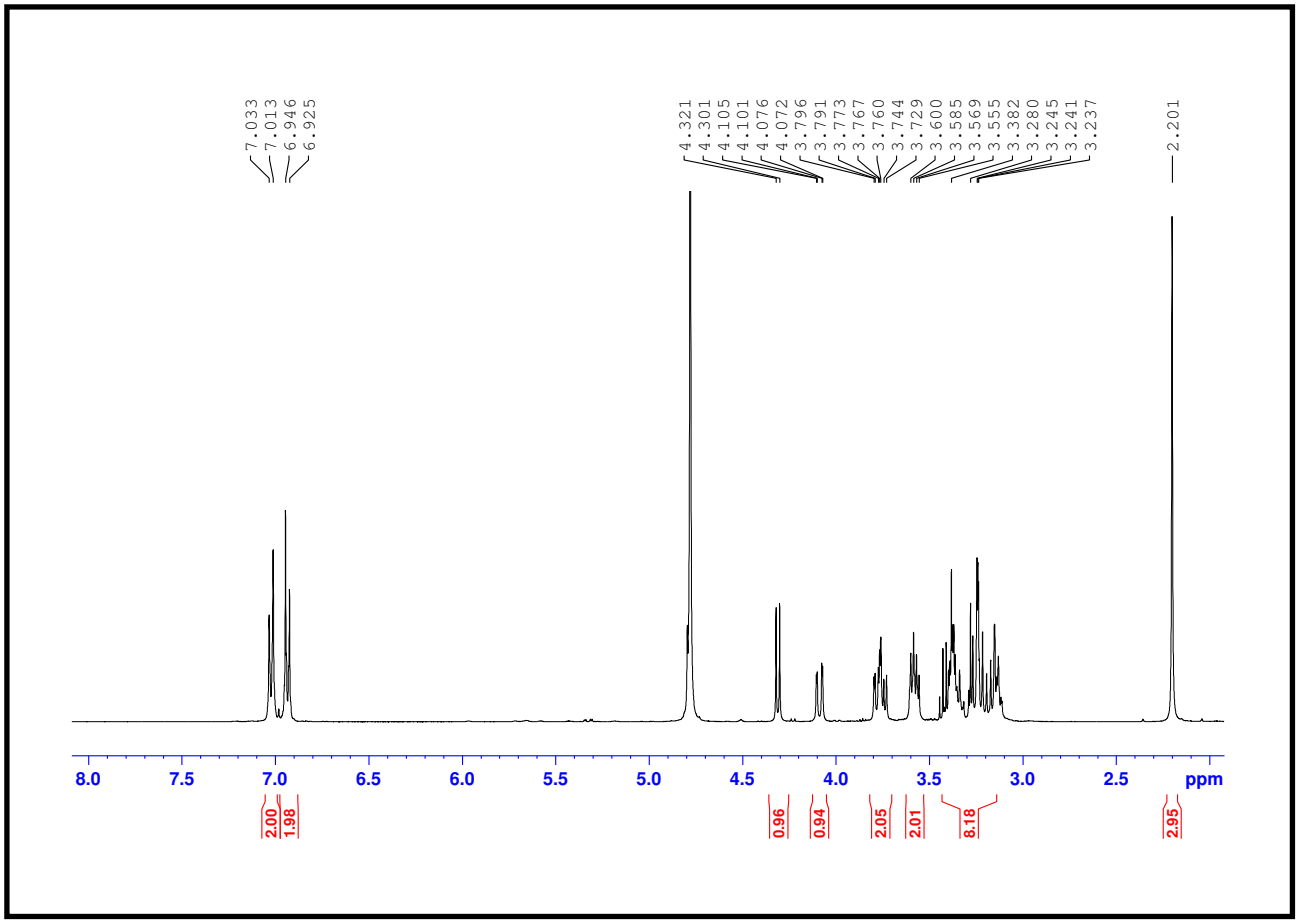

Figure 28 - ^{1}H NMR spectrum of para-cresol gentiobioside

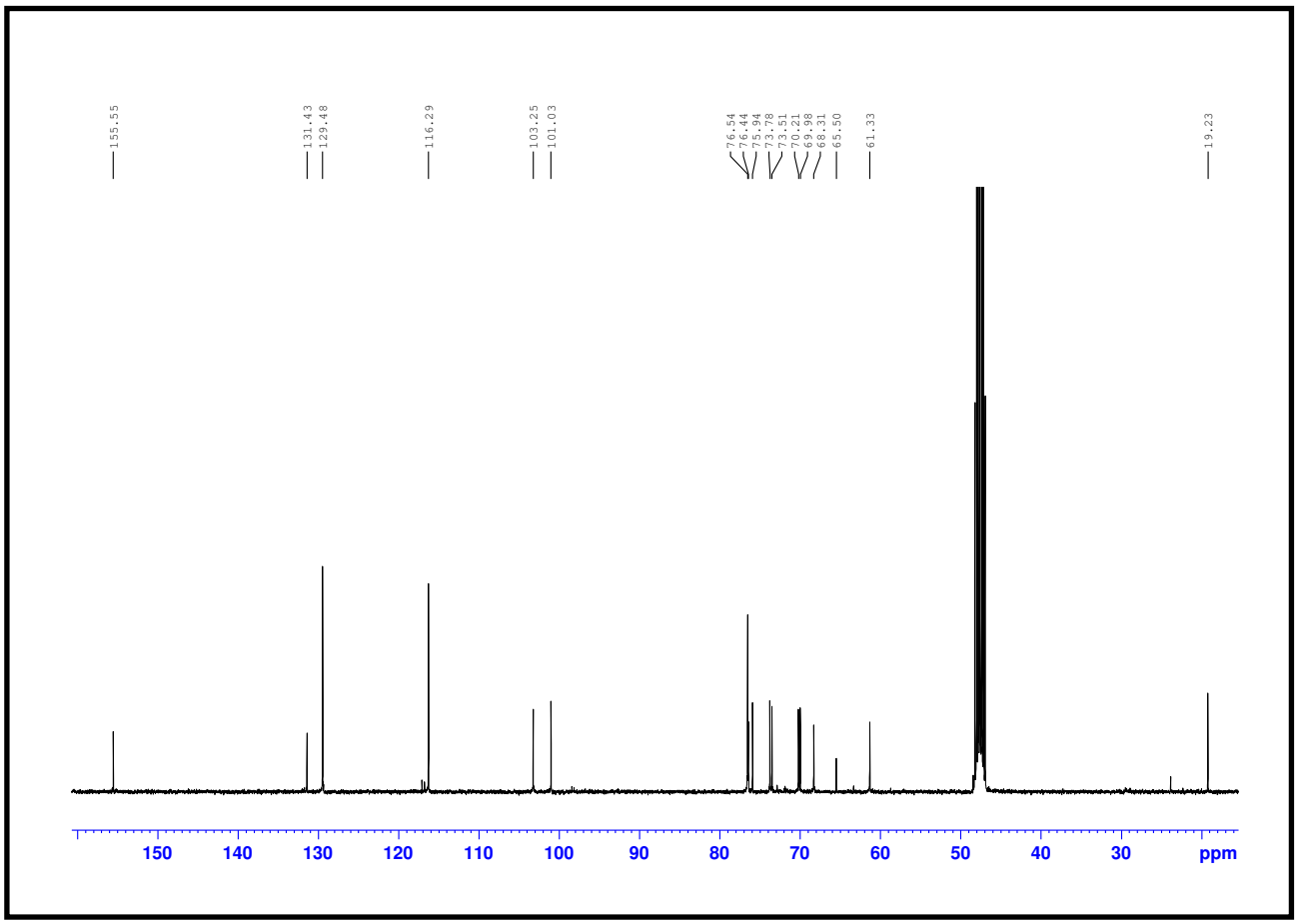

Figure 29 - ^{13}C NMR spectrum of para-cresol gentiobioside

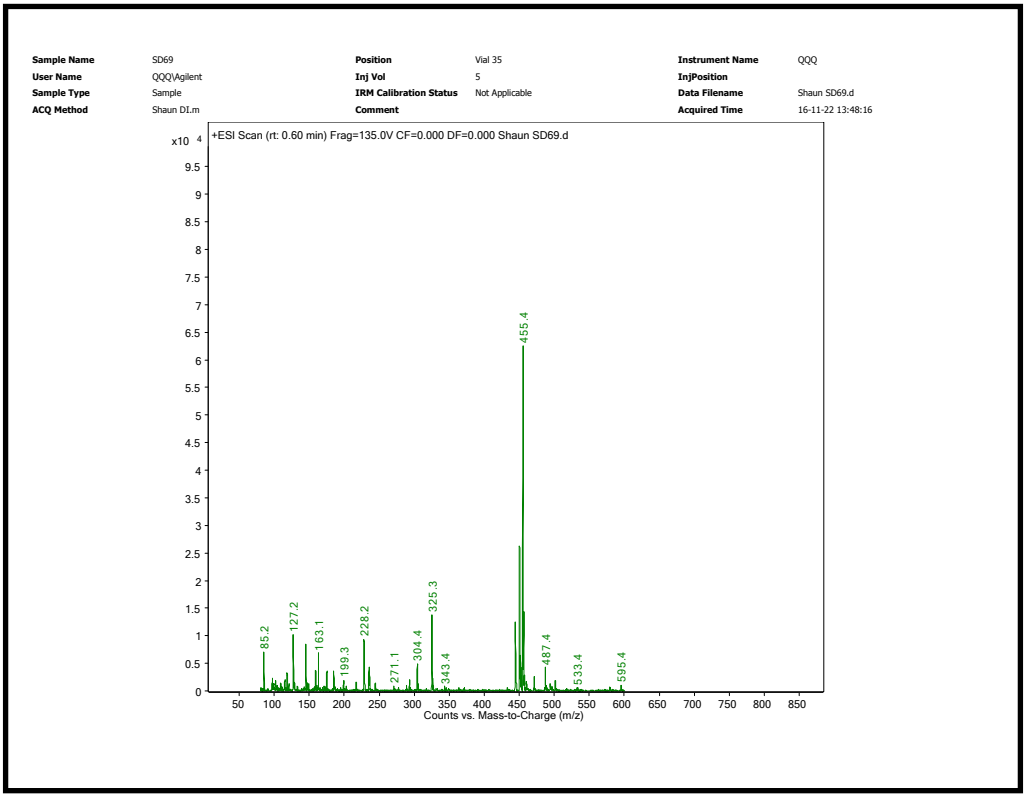

Figure 30 - Low Resolution Mass Spectrum of para-cresol gentiobioside

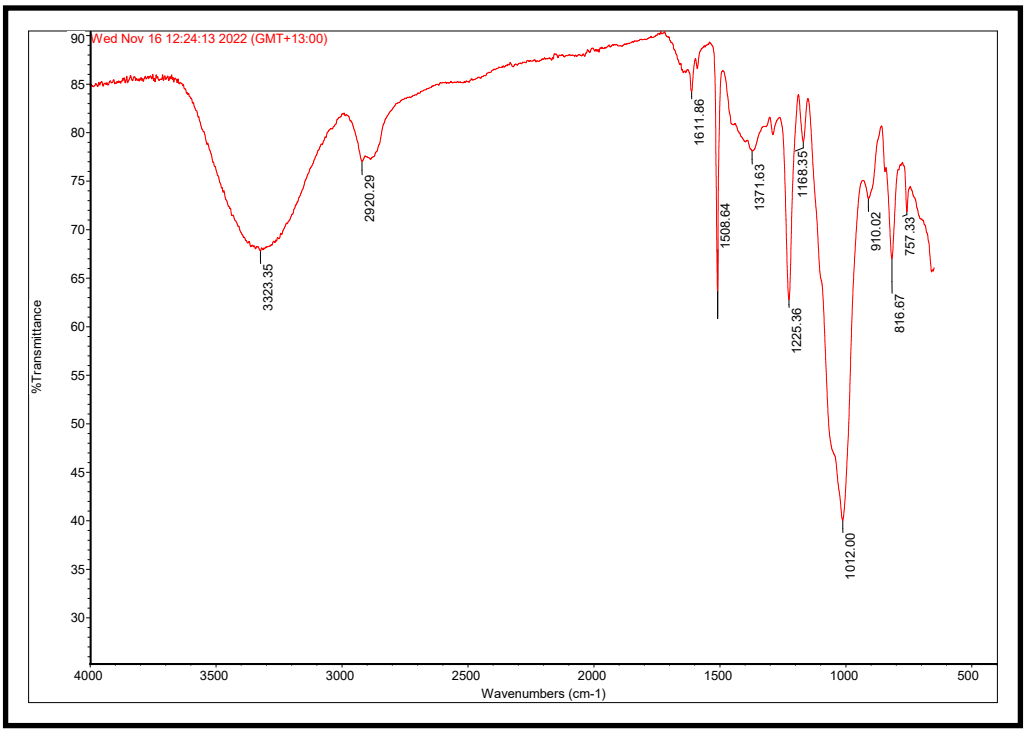

Figure 31 - IR spectrum of para-cresol gentiobioside

2.2 An alternative route for the synthesis of para-cresol

Although the synthesis for para-cresol gentiobioside was successfully completed in this project, the synthetic pathway that was followed was found to be extremely time-consuming and laborious. Due to that reason, in the final stages of this project an alternative synthetic route which was much shorter and more efficient was developed. Figure 32 below shows the new improved synthetic scheme for the synthesis of para-cresol.

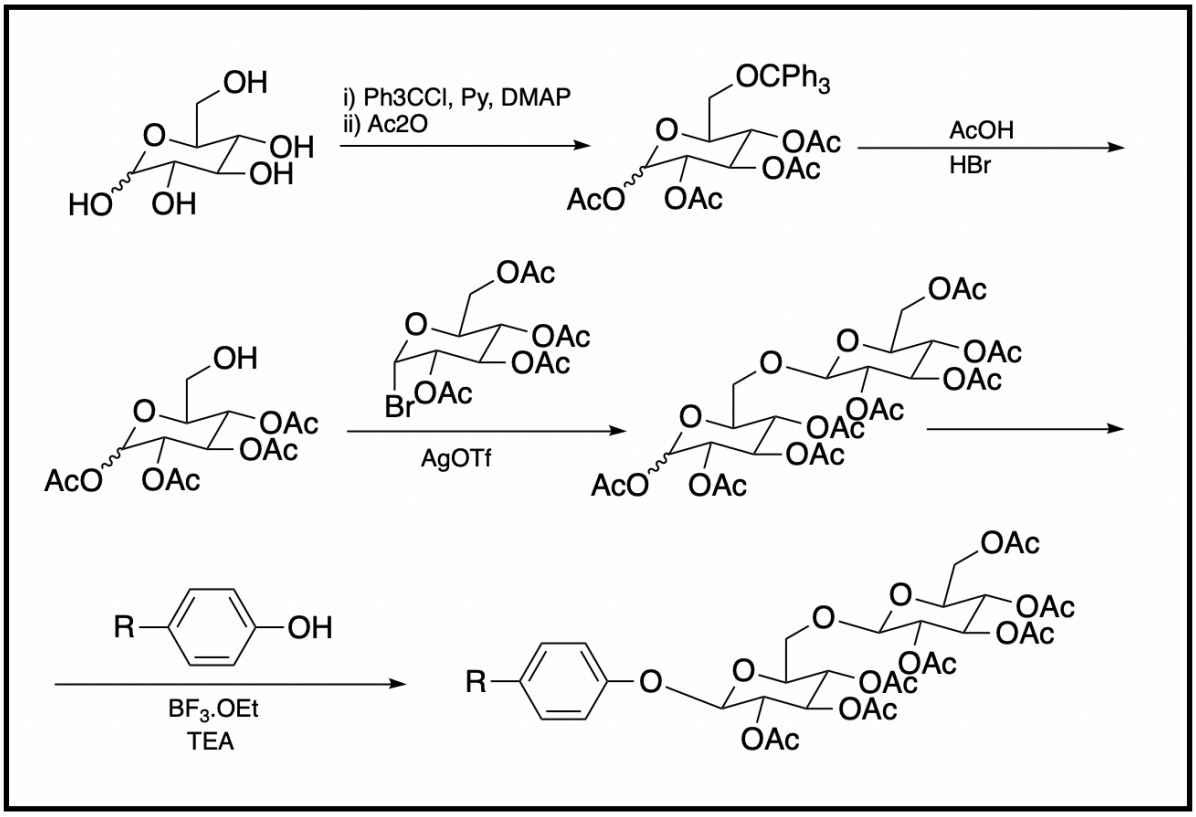

Figure 32 - An alternative synthetic route for para-cresol gentiobioside

Instead of carrying out the synthesis of the target compound on a step by step basis, this new improved synthetic scheme works by first synthesising the disaccharide in bulk quantities to which the volatile phenolic compound can be attached in the last step. In addition to being more efficient, this new synthetic scheme has the added advantage of providing faster access to lots of other phenolic glycosides that are responsible for the presence of smoke taint in wine. This can be achieved by simply varying the type volatile phenolic compound used in the final step. Steps one and two in this synthetic scheme was also a selective protection and de-protection strategy similar to what was performed in the original synthetic scheme. Steps three and four were then two glycosylation reactions, which were also seen before, to attach a second sugar molecule and then finally the phenolic group. Early results from a few different test reactions for the above synthetic route had all looked very promising and showed tremendous potential.

CHAPTER THREE: EXPERIMENTAL

3.1 The synthesis of *para*-cresol gentiobioside

3.1.1 Step I of the synthesis

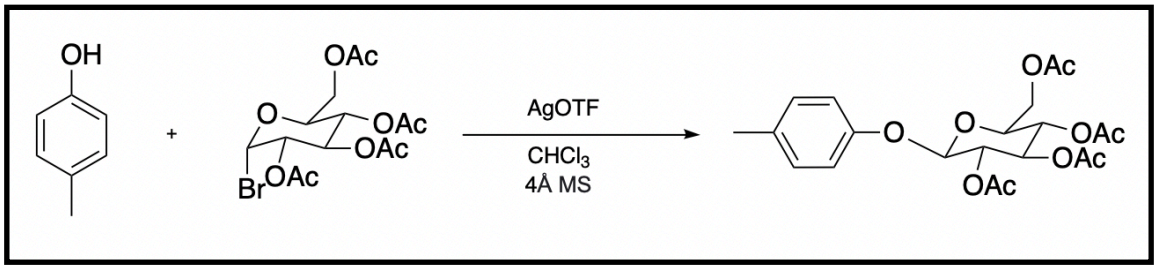

Initially a solution of *p*-cresol (0.600 g, 5.55 mmol), acetobromo-α-D-glucose (2.74 g, 6.66 mmol), and activated 4Å molecular sieves (0.500 g) in chloroform (18 mL) was stirred at 0°C under nitrogen for a period of 10 minutes. Next at 0°C again, silver trifluoromethanesulfonate (1.71 g, 6.66 mmol) was added and the mixture was allowed to stir for an additional 4 hours in the dark. Following the completion of the reaction, the reaction mixture was then quenched with triethylamine (4.2 mL), diluted with chloroform (18 mL) and filtered through a band of celite. Moving on, the crude product was then extracted thrice using chloroform and water. The combined organic layer from the extraction was then dried over $MgSO_4$, filtered, and evaporated under reduced pressure. To end, the mixture was then purified by flash chromatography (100% chloroform for compound loading and slurry preparation, followed by gradient elution from 100% chloroform (500mL) to 1% ethyl acetate in chloroform (300 mL), to 2% ethyl acetate in chloroform (300 mL), and ending with 3% ethyl acetate in chloroform (300 mL)) to obtain the pure compound as a slightly yellowish oil (1.29 g, 53%).

δ_H (400 MHz; CDCl3): 2.03 (3H, s), 2.04 (3H, s), 2.06 (3H, s), 2.08 (3H, s), 2.30 (3H, s), 3.81-3.85 (1H, m), 4.17 (1H, d, *J* = 2, 12 Hz), 4.28 (1H, d, *J* = 5, 12 Hz), 5.02 (1H, d, *J* = 7 Hz), 5.17 (1H, t, *J* = 9 Hz), 5.23-5.30 (2H, m), 6.89 (2H, d, *J* = 9 Hz), 7.09 (2H, d, *J* = 9 Hz)

δC (100 MHz, CDCl3): 20.6, 20.6, 20.6, 20.7, 20.7, 62.0, 68.3, 71.2, 72.0, 72.8, 100.0, 117.0, 130.0, 132.9, 154.8, 169.3, 169.4, 170.3, 170.6

IR vmax(film)/cm^{-1}: 2943, 1741, 1510, 1366, 1256, 1209

The NMR data was in agreement with what was stated in the literature.[33]

3.1.2 Step II of the synthesis

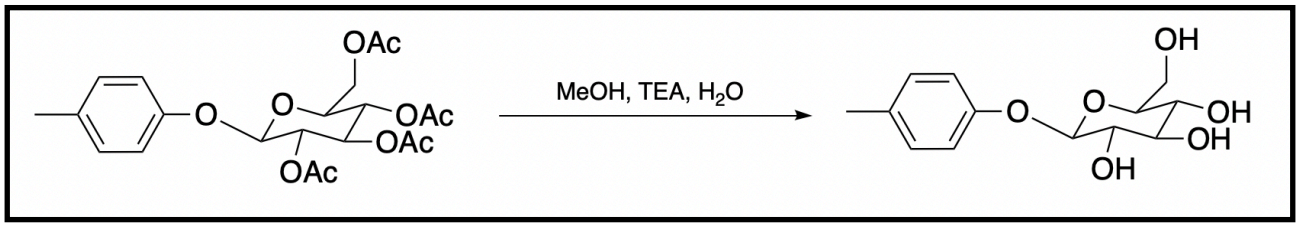

The product from 3.1.1 (1.29 g, 2.94 mmol) was collected and dissolved in a mixture of MeOH-NEt_3-H_2O (8:1:1, 30 mL). The solution was then left to stir at room temperature for a period of 24 hours. In the next step in order to remove triethylamine, the reaction mixture was evaporated under reduced pressure several times with water until there was no further change in the mass of the solid residue. The product was then isolated as a white powder (0.779 g, 98%).

δ_H (400 MHz; CD_3OD): 2.19 (3H, s), 3.23-3.24 (3H, m), 3.28-3.38 (2H, m), 3.62 (1H, d, *J* = 5, 12 Hz), 3.81 (1H, d, *J* = 2, 12 Hz), 6.90 (2H, d, *J* = 9 Hz), 7.00 (2H, d, *J* = 9 Hz).

δ_C (100 MHz, CD_3OD): 20.9, 62.8, 71.7, 75.2, 78.3, 78.4, 102.9, 118.0, 131.1, 133.1, 157.4

IR vmax(film)/cm^{-1}: 3489, 3396, 3240, 2892, 1508, 1226

The NMR data was in agreement with what was stated in the literature.[34]

3.1.3 Step III of the synthesis

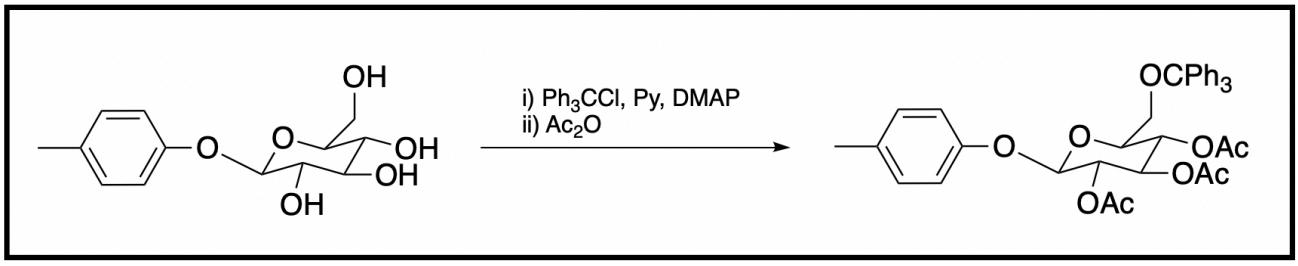

Anhydrous pyridine (2.2 mL, 27.3 mmol) was added under nitrogen to a mixture of the product from 3.1.2 (0.600 g, 2.22 mmol), DMAP (0.00814 g, 0.0666 mmol), and Ph_3CCl (1.07 g, 3.84 mmol). The resulting mixture was then stirred at 60°C for a period of 4 hours. After 4 hours, acetic anhydride (2.2 mL, 23.4 mmol) was added and the mixture was then allowed to stir overnight at room temperature. The reaction was carefully monitored by Thin Layer Chromatography. In the next step, after placing the flask on ice, MeOH (3 mL) was added and the resulting mixture was then let to stir for an additional 30 minutes. Upon removing the solvent under reduced pressure, the crude product was dissolved in DCM and then washed sequentially with 0.1 M HCl, water, and brine. Moving on, the organic layer was then dried over $MgSO_4$, filtered, and then once again evaporated under reduced pressure. In the final step, the mixture was purified by flash chromatography (100% chloroform for compound loading and slurry preparation, followed by gradient elution from 1% ethyl acetate in chloroform (300 mL) to 2% ethyl acetate in chloroform (300 mL) to 3% ethyl acetate in chloroform (600 mL) to yield the title compound (1.22 g, 86%).

δ_H (400 MHz; $CDCl_3$): 1.74 (3H, s), 2.01 (3H, s), 2.08 (3H, s), 2.32 (3H, s), 3.20-3.21 (2H, m), 3.64-3.68 (1H, m), 5.00 (1H, d, *J* = 8 Hz), 5.13 (1H, t, *J* = 9 Hz), 5.21 (1H, t, *J* = 9 Hz), 5.29 (1H, t, *J* = 8 Hz), 7.03 (2H, d, *J* = 9 Hz), 7.10 (2H, d, *J* = 9 Hz), 7.20-7.29 (10H, m), 7.43-7.46 (5H, m)

δ_C (100 MHz, $CDCl_3$): 20.4, 20.7, 20.7, 62.1, 68.7, 71.4, 73.0, 73.7, 86.8, 100.0, 117.4, 127.0, 127.8, 128.9, 130.0, 132.7, 143.5, 155.0, 169.0, 169.4, 170.0

3.1.4 Step IV of the synthesis

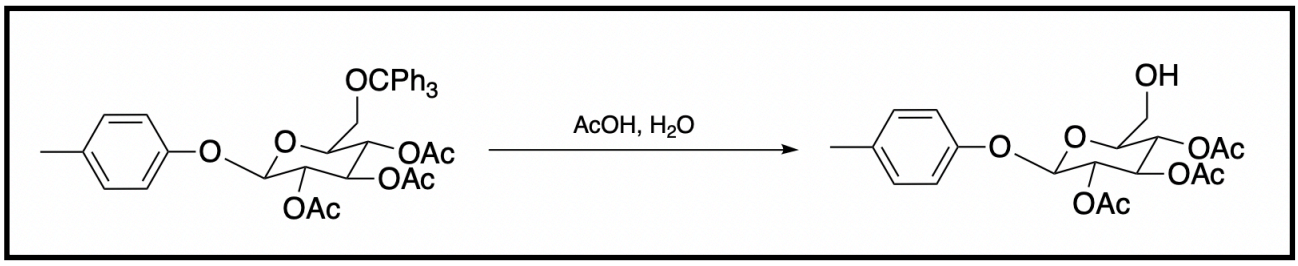

The product from 3.1.3 (0.868 g, 1.36 mmol) was dissolved in a mixture of HOAc-H_2O (4:1, 40 mL). The resultant solution was then stirred at 100°C under reflux for 2 hours. After cooling to room temperature, the mixture was then allowed to stir overnight at room temperature. In the next step, the resulting crystals were then filtered and given a wash using 75% MeOH (15 mL). The filtrate and the washings were then combined and evaporated under reduced pressure to give a residue. The residue was then purified using flash chromatography to give the title compound (0.290 g, 54%).

δ_H (400 MHz; $CDCl_3$): 2.04 (3H, s), 2.05 (3H, s), 2.07 (3H, s), 2.30 (3H, s), 3.61-3.68 (2H, m), 3.73-3.80 (1H, m), 5.08-5.13 (2H, m), 5.23 (1H, t, *J* = 9 Hz), 5.33 (1H, t, *J* = 9 Hz), 6.88 (2H, d, *J* = 9 Hz), 7.10 (2H, d, *J* = 9 Hz)

δC (100 MHz, $CDCl_3$): 20.6, 20.6, 20.8, 20.8, 61.4, 69.0, 70.9, 71.2, 74.0, 97.1, 117.3, 129.0, 130.2, 155.0, 169.3, 169.4, 170.1

3.1.5 Step V of the synthesis

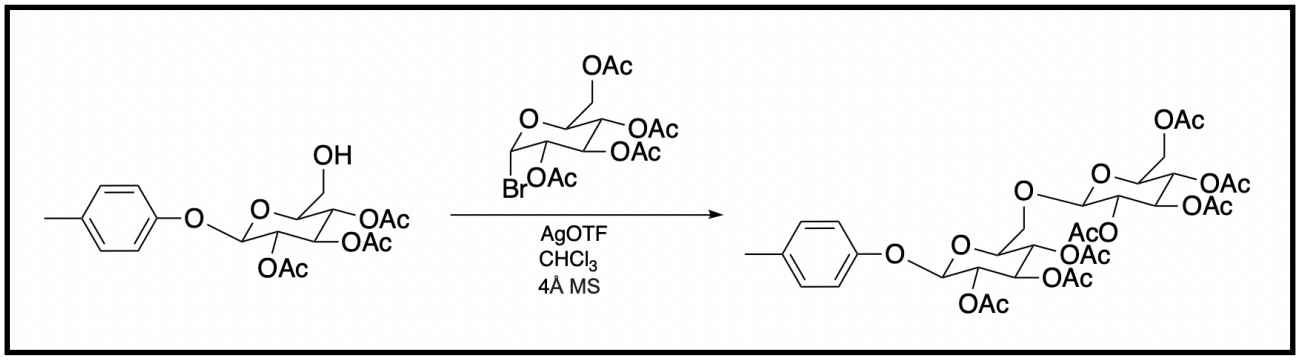

A solution of acetobromo-α-D-glucose (0.600 g, 1.46 mmols) in $CHCl_3$ (25 mL) was added dropwise in the dark to a stirred solution of the product from 3.1.4 (0.290 g, 0.73 mmols), silver trifluoromethanesulfonate (0.417 g, 1.62 mmols), and 4Å molecular sieves (0.600 g) in $CHCl_3$ (25 mL). In the next step, the reaction was then allowed to stir for a period of 2 hours. The reaction was carefully monitored by Thin Layer Chromatography. Upon completion the reaction was quenched with Et_3N, diluted with $CHCl_3$, and then filtered through a funnel packed with celite. In the final step, flash chromatography (20% EtOAc in $CHCl_3$) gave the pure compound (0.154 g, 29%) as an off-white solid.

δ_H (400 MHz; $CDCl_3$): 1.87 (3H, s), 2.00 (3H, s), 2.01 (3H, s), 2.02 (3H, s), 2.04 (3H ,s), 2.05 (3H, s), 2.08 (3H, s), 2.32 (3H, s), 3.52-3.56 (1H, m), 3.66-3.71 (1H, m), 3.81-3.86 (2H, m), 4.10 (1H, d, *J* = 2, 12 Hz), 4.23 (1H, d, *J* = 5, 12 Hz), 4.57 (1H, d, *J* = 8 Hz), 4.92-5.30 (7H, m), 6.88 (2H, d, *J* = 9 Hz), 7.14 (2H, d, *J* = 9 Hz)

δ_C (100 MHz, $CDCl_3$): 20.4, 20.5, 20.5, 20.5, 20.5, 20.6, 61.6, 67.7, 68.2, 68.7, 71.1, 71.1, 71.8, 72.5, 72.7, 74.0, 99.0, 100.3, 116.4, 130.2, 132.8, 154.7, 169.3, 169.3, 169.6, 170.0, 170.1, 170.5

3.1.6 Step VI of the synthesis

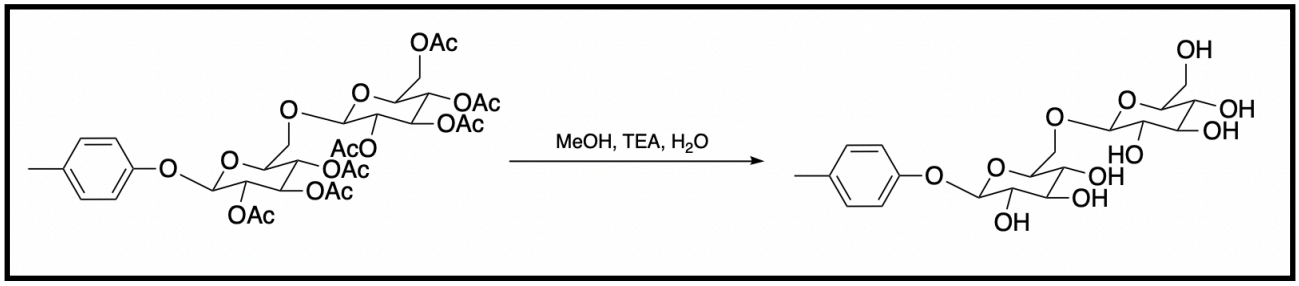

The product from 3.1.5 (0.130 g, 0.179 mmols) was collected and dissolved in a mixture of MeOH-NEt_3-H_2O (8:1:1, 10 mL). In the next step, the solution was allowed to stir at room temperature for a period of 24 hours. On completion of the 24 hour period, the reaction mixture was then repeatedly evaporated with water under reduced pressure until the mass of the solid residue remained unchanged. The product (0.0750 g, 97%) was then obtained as a slightly yellow oil.

δ_H (400 MHz; CD_3OD): 2.20 (3H, s), 3.11-3.45 (8H, m), 3.56-3.60 (2H, m), 3.73-3.80 (2H, m), 4.09 (1H, d, *J* = 2, 12 Hz), 4.31 (1H, d, *J* = 8 Hz), 6.93 (2H, d, *J* = 9 Hz), 7.02 (2H, d, *J* = 9 Hz)

δ_C (100 MHz, CD_3OD): 19.2, 61.3, 65.5, 68.3, 70.0, 70.2, 73.5, 73.8, 75.9, 76.4, 76.5, 101.0, 103.2, 116.3, 129.5, 131.4, 155.5

IR vmax(film)/cm^{-1}: 3323, 2920, 1611, 1509, 1225, 1012.

MS found (ESI): $[M+Na]^+$, 455.4, $C_{19}H_{28}NaO_{11}$ requires 455.4

CHAPTER FOUR : CONCLUSIONS AND FUTURE WORK

The main aim of this project was to synthesise the novel compound para-cresol, which is one of many compounds that are responsible for the presence of smoke taint in wine. All reactions from the proposed synthetic scheme for para-cresol gentiobioside were carried out and optimised where required to improve the % yield of the product. 0.0750 grams of the novel compound para-cresol was successfully synthesised and purified. The final pure product will be utilised, by the industrial collaborators that were involved in this project, for the development of molecularly imprinted polymers in order to selectively remove the same compound, or other closely related analogues from smoke-tainted wine. Future work would involve developing the new improved synthetic route described in section 2.2, which when completed will allow for faster and more streamlined access to a range of other different smoke-taint compounds. Figure 33 below shows a few examples of some of the other important smoke-taint compounds. Once synthesised, these molecules can be used to develop even more molecularly imprinted polymers, which could potentially be a lasting solution to the problem of smoke-tainted wine.

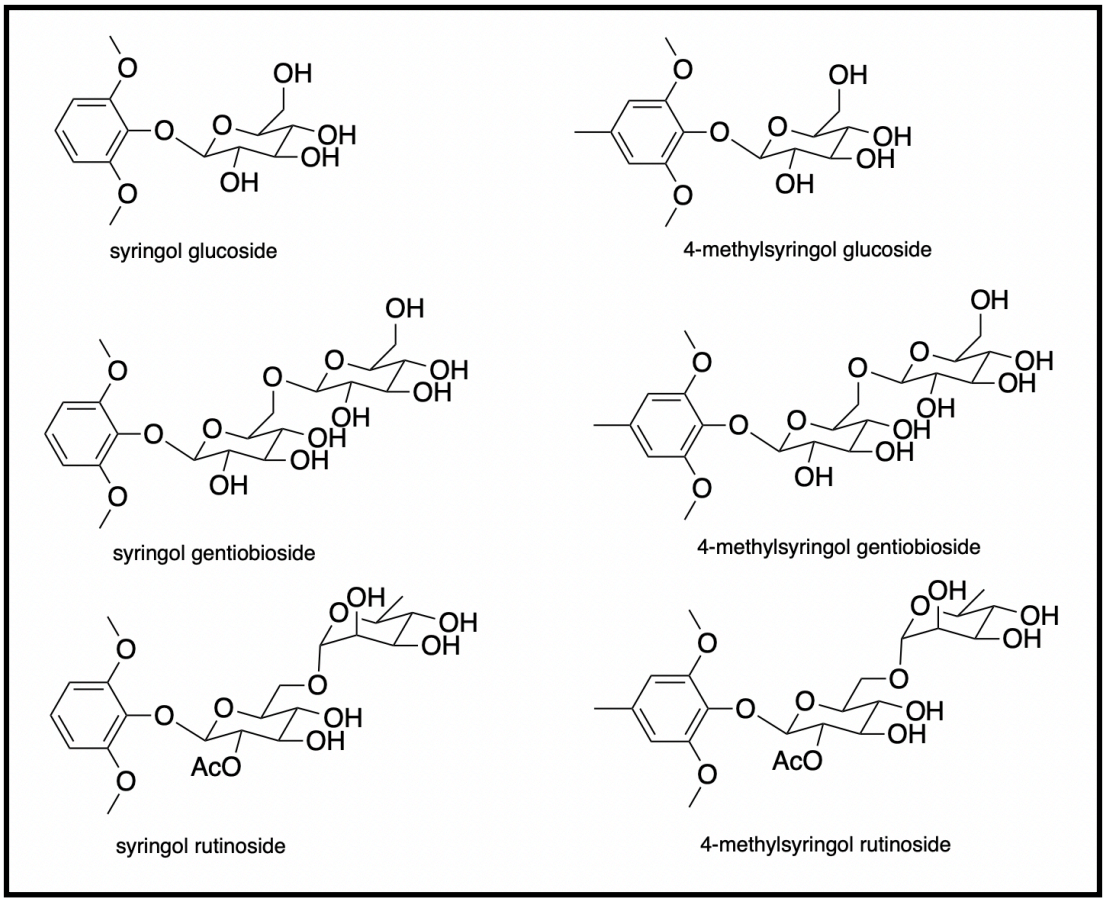

Figure 33 - Examples of other smoke-taint related compounds

References

(1)
Mirabelli-Montan, Y. A.; Marangon, M.; Graça, A.; Mayr Marangon, C. M.; Wilkinson, K. L. Techniques for Mitigating the Effects of Smoke Taint While Maintaining Quality in Wine Production: A Review. *Molecules* **2021**, *26* (6), 1672. https://doi.org/10.3390/molecules26061672.
(2)
Overpeck, J. T.; Rind, D.; Goldberg, R. Climate-Induced Changes in Forest Disturbance and Vegetation. *Nature* **1990**, *343* (6253), 51–53. https://doi.org/10.1038/343051a0.
(3)
Mozell, M. R.; Thach, L. The Impact of Climate Change on the Global Wine Industry: Challenges & Solutions. *Wine Economics and Policy* **2014**, *3* (2), 81–89. https://doi.org/10.1016/j.wep.2014.08.001.
(4)
Kennison, K. R.; Gibberd, M. R.; Pollnitz, A. P.; Wilkinson, K. L. Smoke-Derived Taint in Wine: The Release of Smoke-Derived Volatile Phenols during Fermentation of Merlot Juice Following Grapevine Exposure to Smoke. *Journal of Agricultural and Food Chemistry* **2008**, *56* (16), 7379–7383. https://doi.org/10.1021/jf800927e.
(5)
Krstic, M. P.; Johnson, D. L.; Herderich, M. J. Review of Smoke Taint in Wine: Smoke-Derived Volatile Phenols and Their Glycosidic Metabolites in Grapes and Vines as Biomarkers for Smoke Exposure and Their Role in the Sensory Perception of Smoke Taint. *Australian Journal of Grape and Wine Research* **2015**, *21*, 537–553. https://doi.org/10.1111/ajgw.12183.
(6)
Hayasaka, Y.; Baldock, G. A.; Pardon, K. H.; Jeffery, D. W.; Herderich, M. J. Investigation into the Formation of Guaiacol Conjugates in Berries and Leaves of Grapevine Vitis Vinifera L. Cv. Cabernet Sauvignon Using Stable Isotope Tracers Combined with HPLC-MS and MS/MS Analysis. *Journal of Agricultural and Food Chemistry* **2010**, *58* (4), 2076–2081. https://doi.org/10.1021/jf903732p.
(7)
KENNISON, K. R.; WILKINSON, K. L.; POLLNITZ, A. P.; WILLIAMS, H. G.; GIBBERD, M. R. Effect of Timing and Duration of Grapevine Exposure to Smoke on the Composition and Sensory Properties of Wine. *Australian Journal of Grape and Wine Research* **2009**, *15* (3), 228–237. https://doi.org/10.1111/j.1755-0238.2009.00056.x.
(8)
Caffrey, A.; Lerno, L.; Rumbaugh, A.; Girardello, R.; Zweigenbaum, J.; Oberholster, A.; Ebeler, S. E. Changes in Smoke-Taint Volatile-Phenol Glycosides in Wildfire Smoke-Exposed Cabernet Sauvignon Grapes throughout Winemaking. *American Journal of Enology and Viticulture* **2019**, ajev.2019.19001. https://doi.org/10.5344/ajev.2019.19001.

(9)
Pollnitz, A. P.; Pardon, K. H.; Sykes, M.; Sefton, M. A. The Effects of Sample Preparation and Gas Chromatograph Injection Techniques on the Accuracy of Measuring Guaiacol, 4-Methylguaiacol and Other Volatile Oak Compounds in Oak Extracts by Stable Isotope Dilution Analyses. *Journal of Agricultural and Food Chemistry* **2004**, *52* (11), 3244–3252. https://doi.org/10.1021/jf035380x.
(10)
Noestheden, M.; Dennis, E. G.; Zandberg, W. F. Quantitating Volatile Phenols in Cabernet Franc Berries and Wine after On-Vine Exposure to Smoke from a Simulated Forest Fire. *Journal of Agricultural and Food Chemistry* **2018**, *66* (3), 695–703. https://doi.org/10.1021/acs.jafc.7b04946.
(11)
Turiel, E.; Esteban, A. M. Molecularly Imprinted Polymers. *Solid-Phase Extraction* **2020**, 215–233. https://doi.org/10.1016/b978-0-12-816906-3.00008-x.
(12)
Vasapollo, G.; Sole, R. D.; Mergola, L.; Lazzoi, M. R.; Scardino, A.; Scorrano, S.; Mele, G. Molecularly Imprinted Polymers: Present and Future Prospective. *International Journal of Molecular Sciences* **2011**, *12* (9), 5908–5945. https://doi.org/10.3390/ijms12095908.
(13)
Board, E.; Houk; Hunter, C.; Krische, M.; Lehn, J.-M.; Ley, S.; Olivucci, M.; Thiem, J.; Venturi, M.; Vogel, P.; Wong, C.-H.; Wong, H.; Yamamoto, H. *Topics in Current Chemistry*.
(14)
Das, R.; Mukhopadhyay, B. Chemical O-Glycosylations: An Overview. *ChemistryOpen* **2016**, *5* (5), 401–433. https://doi.org/10.1002/open.201600043.

(15)
Wood, E. J. Biochemistry: The Chemical Reactions of Living Cells. *Biochemistry and Molecular Biology Education* **2004**, *32* (1), 62–63. https://doi.org/10.1002/bmb.2004.494032010298.
(16)
Munro, S. Essentials of Glycobiology. *Trends in Cell Biology* **2000**, *10* (12), 552–553. https://doi.org/10.1016/s0962-8924(00)01855-9.
(17)
Kiessling, L. L.; Splain, R. A. Chemical Approaches to Glycobiology. *Annual Review of Biochemistry* **2010**, *79* (1), 619–653. https://doi.org/10.1146/annurev.biochem.77.070606.100917.
(18)
Sánchez-Fernández, E. M.; Rísquez-Cuadro, R.; Ortiz Mellet, C.; García Fernández, J. M.; Nieto, P. M.; Angulo, J. Sp ^{2} -Iminosugar *O* -, *S* -, and *N* -Glycosides as Conformational Mimics of α-Linked Disaccharides; Implications for Glycosidase Inhibition. *Chemistry – A European Journal* **2012**, *18* (27), 8527–8539. https://doi.org/10.1002/chem.201200279.

(19)
Somsák, L. Carbanionic Reactivity of the Anomeric Center in Carbohydrates. *Chemical Reviews* **2001**, *101* (1), 81–136. https://doi.org/10.1021/cr980007n.
(20)
Jarosz, S. Editorial (Thematic Issue: Simple Sugars in Organic Synthesis: The Stereochemical and Biological Aspects: Part-I). *Current Organic Chemistry* **2014**, *18* (13), 1673–1673. https://doi.org/10.2174/1385272818131409041559 29.
(21)
Waldvogel, S. R. The Organic Chemistry of Sugars. *Synthesis* **2007**, *2007* (3), 484–484. https://doi.org/10.1055/s-2007-970124.
(22)
Nukada, T.; Bérces, A.; Whitfield, D. M. Can the Stereochemical Outcome of Glycosylation Reactions Be Controlled by the Conformational Preferences of the Glycosyl Donor? *Carbohydrate Research* **2002**, *337* (8), 765–774. https://doi.org/10.1016/s0008-6215(02)00043-5.
(23)
Karak, M.; Joh, Y.; Suenaga, M.; Oishi, T.; Torikai, K. 1,2-*Trans* Glycosylation via Neighboring Group Participation of 2-*O*-Alkoxymethyl Groups: Application to One-Pot Oligosaccharide Synthesis. *Organic Letters* **2019**, *21* (4), 1221–1225. https://doi.org/10.1021/acs.orglett.9b00220.
(24)
Cox, D. J.; Singh, G. P.; Watson, A. J. A.; Fairbanks, A. J. Neighbouring Group Participation during Glycosylation: Do 2-Substituted Ethyl Ethers Participate? *European Journal of Organic Chemistry* **2014**, *2014* (21), 4624–4642. https://doi.org/10.1002/ejoc.201402260.
(25)
Demchenko, A. V. 1,2-Cis O-Glycosylation: Methods, Strategies, Principles. *Current Organic Chemistry 7* (1), 35–79.
(26)
Nigudkar, S. S.; Demchenko, A. V. Stereocontrolled 1,2-Cis Glycosylation as the Driving Force of Progress in Synthetic Carbohydrate Chemistry. *Chemical Science* **2015**, *6* (5), 2687–2704. https://doi.org/10.1039/c5sc00280j.
(27)
Guo, J.; Ye, X.-S. Protecting Groups in Carbohydrate Chemistry: Influence on Stereoselectivity of Glycosylations. *Molecules* **2010**, *15* (10), 7235–7265. https://doi.org/10.3390/molecules15107235.
(28)
Toshima, K. Glycosyl Halides and Anomeric Esters as Donors. *ChemInform* **2003**, *34* (2). https://doi.org/10.1002/chin.200302246.

(29)
Flowers, H. M. Studies on the Koenigs-Knorr Reaction. *Carbohydrate Research* **1971**, *18* (2), 211–218. https://doi.org/10.1016/s0008-6215(00)80344-4.
(30)
Li, Y.-W.; Ma, C.-L. Improved Synthesis of Gastrodin, a Bioactive Component of a Traditional Chinese Medicine. *Journal of the Serbian Chemical Society* **2014**, *79* (10), 1205–1212.
(31)
Shao, Y.; Li, Y.; Zhou, B. PHENOLIC and TRITERPENOID GLYCOSIDES from ASTER BA TANGENSIS. *Phytochemistry* **1996**, *41* (6), 1593–1598.
(32)
Miljković, M. Relative Reactivity of Hydroxyl Groups in Monosaccharides. *Carbohydrates* **2009**, 113–142. https://doi.org/10.1007/978-0-387-92265-2_5.
(33)
Li, Y.-W.; Ma, C.-L. Improved Synthesis of Gastrodin, a Bioactive Component of a Traditional Chinese Medicine. *Journal of the Serbian Chemical Society* **2014**, *79* (10), 1205–1212. https://doi.org/10.2298/jsc131011026l.
(34)
Sahin-Tóth, M.; Gunawan, P.; Lawrence, M. C.; Toyokuni, T.; Kaback, H. R. Binding of Hydrophobic D-Galactopyranosides to the Lactose Permease of *Escherichia Coli*. *Biochemistry* **2002**, *41* (43), 13039–13045. https://doi.org/10.1021/bi0203076.

Appendices

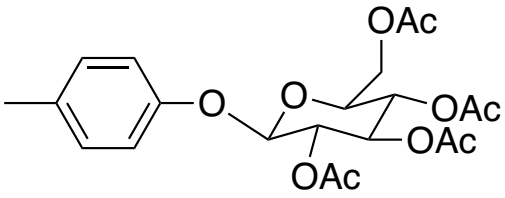
OAc
O
O
OAc
OAc
OAc

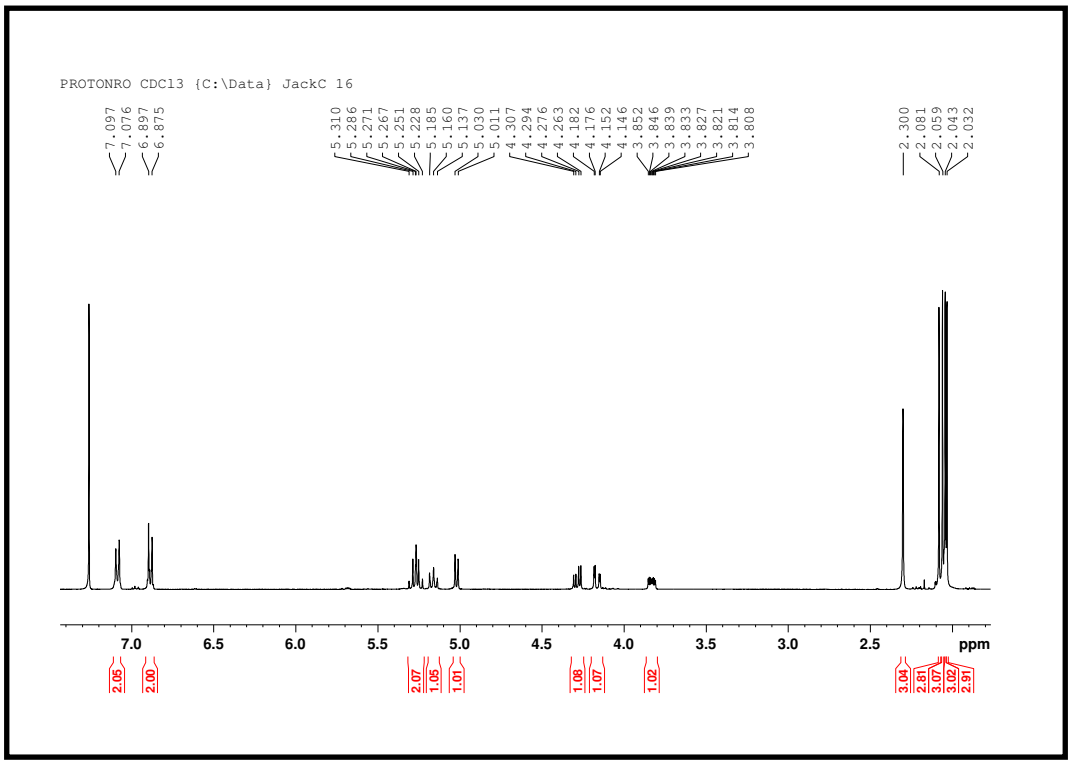
PROTONRO CDCl3 {C:\Data} JackC 16
7.097
7.076
6.897
6.875
5.310
5.286
5.271
5.267
5.251
5.228
5.185
5.160
5.137
5.030
5.011
4.307
4.294
4.276
4.263
4.182
4.176
4.152
4.146
3.852
3.846
3.839
3.833
3.827
3.821
3.814
3.808
2.300
2.081
2.059
2.043
2.032
7.0
6.5
6.0
5.5
5.0
4.5
4.0
3.5
3.0
2.5
ppm
2.05
2.00
2.07
1.05
1.01
1.08
1.07
1.02
3.04
2.81
3.07
3.02
2.91

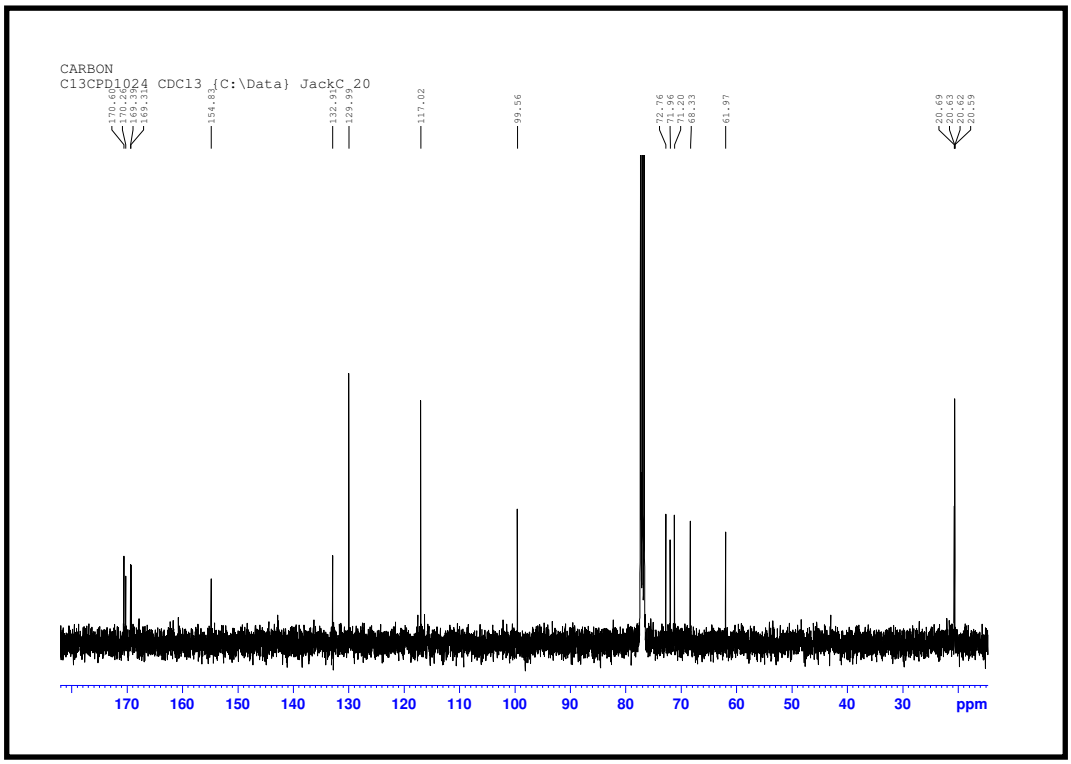
CARBON
C13CPD1024 CDCl3 {C:\Data} JackC 20
170.60
170.26
169.38
169.31
154.83
132.91
129.99
117.02
99.56
72.76
71.96
71.20
63.33
61.97
20.69
20.63
20.62
20.59
170
160
150
140
130
120
110
100
90
80
70
60
50
40
30
ppm

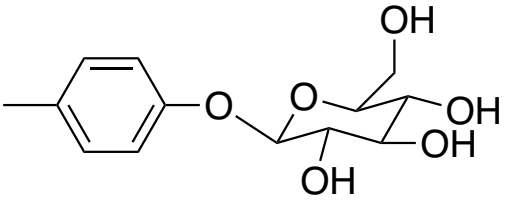
OH
O
O
OH
OH
OH

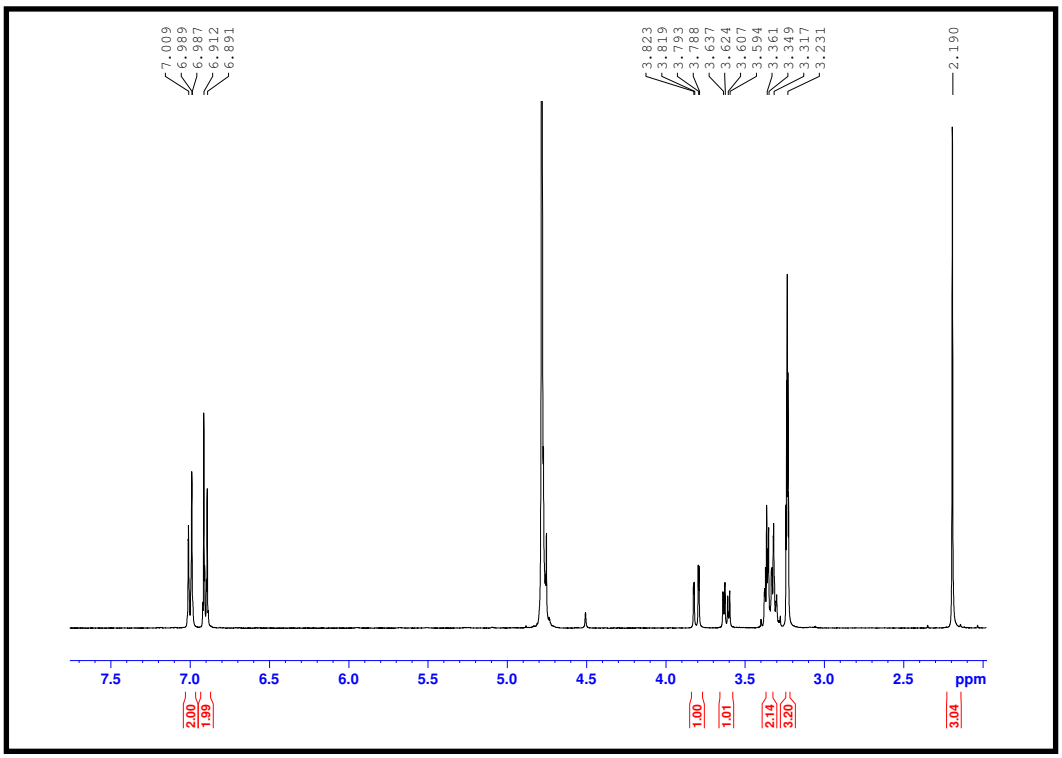
7.009
6.989
6.987
6.912
6.891
3.823
3.819
3.793
3.788
3.637
3.624
3.607
3.594
3.361
3.349
3.317
3.231
2.190
7.5
7.0
6.5
6.0
5.5
5.0
4.5
4.0
3.5
3.0
2.5
ppm
2.00
1.99
1.00
1.01
2.14
3.20
3.04

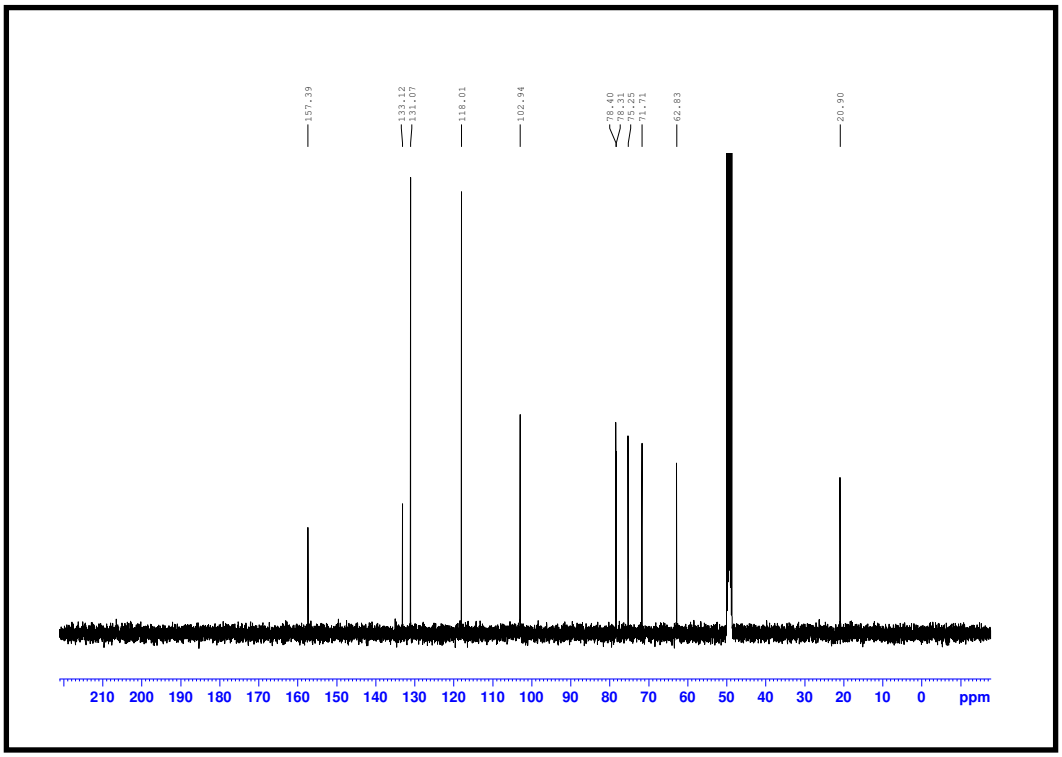
157.39
133.12
131.07
118.01
102.94
78.40
78.31
75.35
71.71
62.83
20.90
210
200
190
180
170
160
150
140
130
120
110
100
90
80
70
60
50
40
30
20
10
0
ppm

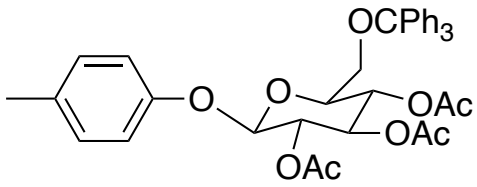
OCPh3
O
O
OAc
OAc
OAc

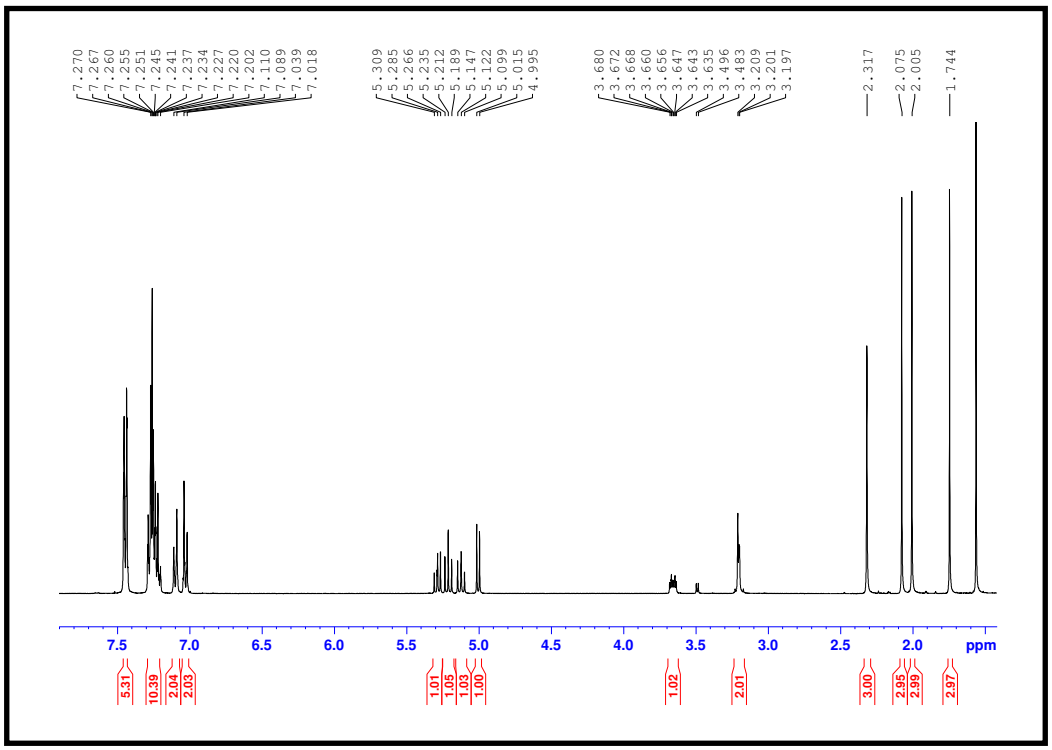
7.270
7.267
7.260
7.255
7.251
7.245
7.241
7.237
7.234
7.227
7.220
7.202
7.110
7.089
7.039
7.018
5.309
5.285
5.266
5.235
5.212
5.189
5.147
5.122
5.099
5.015
4.995
3.680
3.672
3.668
3.660
3.656
3.647
3.643
3.635
3.496
3.483
3.209
3.201
3.197
2.317
2.075
2.005
1.744
7.5
7.0
6.5
6.0
5.5
5.0
4.5
4.0
3.5
3.0
2.5
2.0
ppm
5.31
10.39
2.04
2.03
1.01
1.05
1.03
1.00
1.02
2.01
3.00
2.95
2.99
2.97

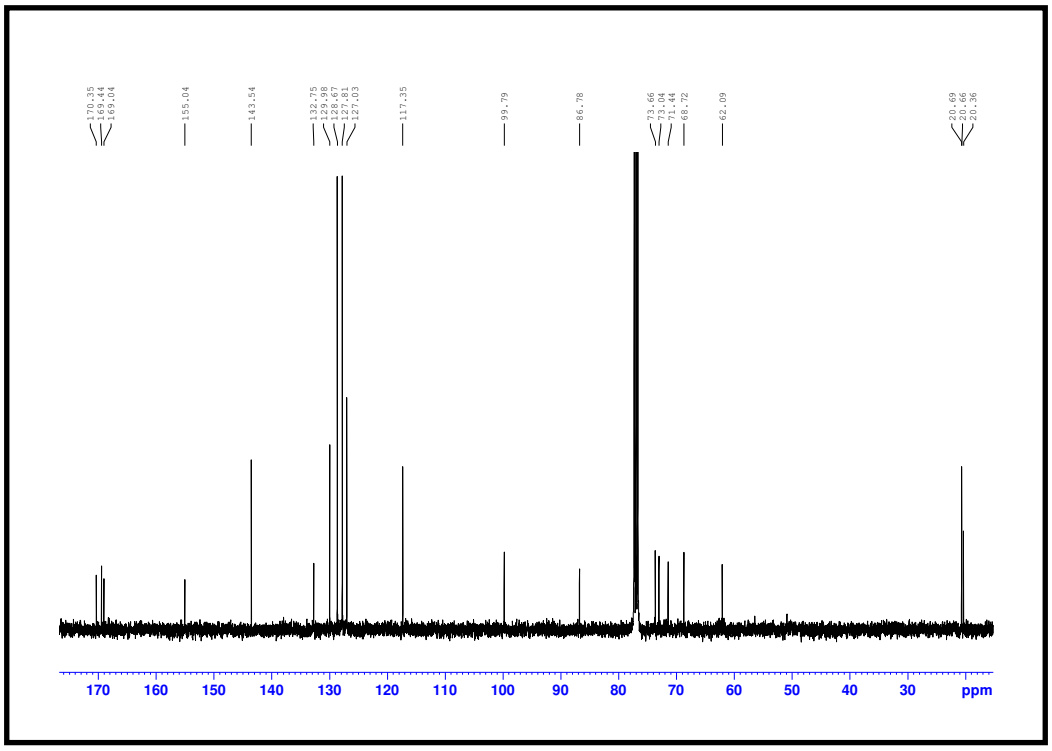
170.35
169.44
169.04
155.04
143.54
132.75
129.98
128.77
127.81
127.03
117.35
99.79
86.78
73.66
73.04
71.44
68.72
62.09
20.69
20.66
20.36
170
160
150
140
130
120
110
100
90
80
70
60
50
40
30
ppm

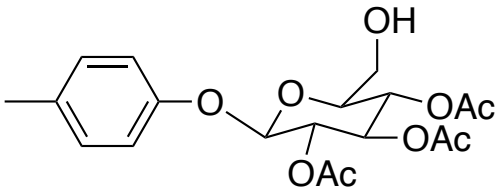
OH
O
O
OAc
OAc
OAc

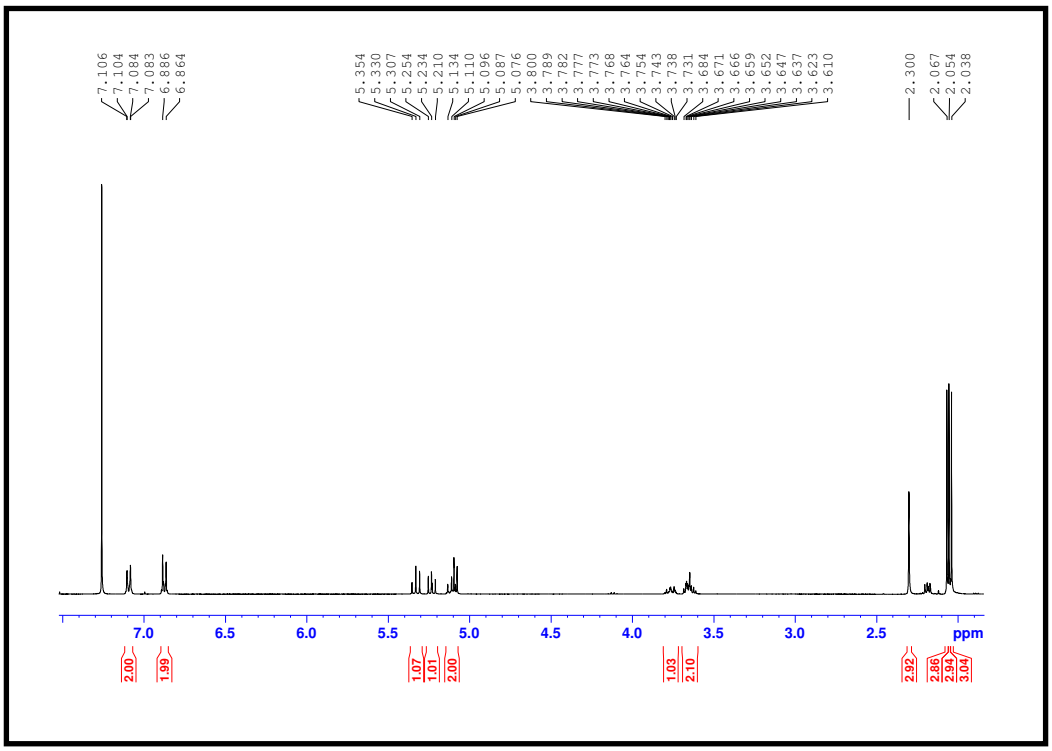
7.106
7.104
7.084
7.083
6.886
6.864
5.354
5.330
5.307
5.254
5.234
5.210
5.134
5.110
5.096
5.087
5.076
3.800
3.789
3.782
3.777
3.773
3.768
3.764
3.754
3.743
3.738
3.731
3.684
3.671
3.666
3.659
3.652
3.647
3.637
3.623
3.610
2.300
2.067
2.054
2.038
7.0
6.5
6.0
5.5
5.0
4.5
4.0
3.5
3.0
2.5
ppm
2.00
1.99
1.07
1.01
2.00
1.03
2.10
2.92
2.86
2.94
3.04

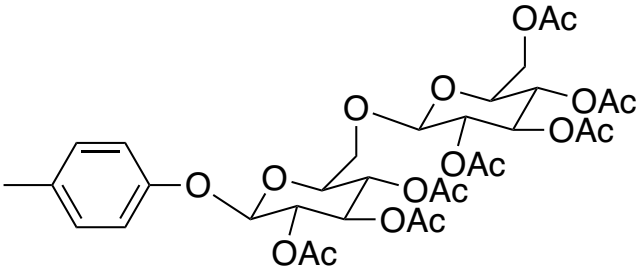
OAc
O
OAc
O
OAc
OAc
O
O
OAc
OAc
OAc

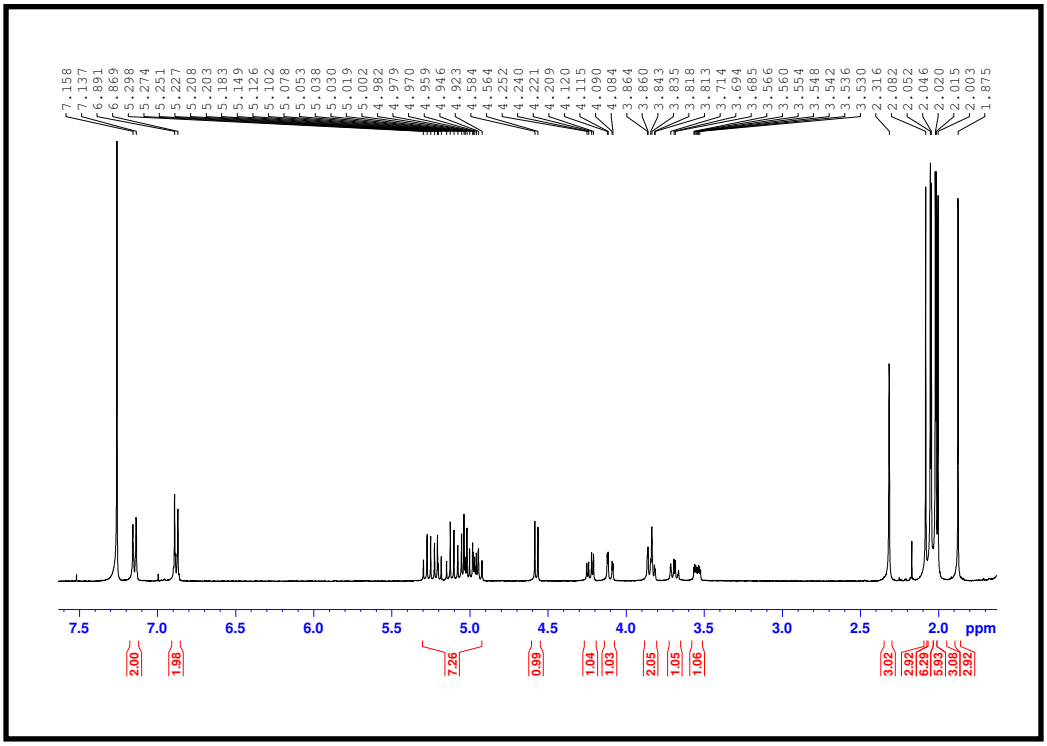
7.158
7.137
6.891
6.869
5.298
5.274
5.251
5.227
5.208
5.203
5.183
5.149
5.126
5.102
5.078
5.053
5.038
5.030
5.019
5.002
4.982
4.979
4.970
4.959
4.946
4.923
4.584
4.564
4.252
4.240
4.221
4.209
4.120
4.115
4.090
4.084
3.864
3.860
3.843
3.835
3.818
3.813
3.714
3.694
3.685
3.566
3.560
3.554
3.548
3.542
3.536
3.530
2.316
2.082
2.052
2.046
2.020
2.015
2.003
1.875
7.5
7.0
6.5
6.0
5.5
5.0
4.5
4.0
3.5
3.0
2.5
2.0
ppm
2.00
1.98
7.26
0.99
1.04
1.03
2.05
1.05
1.06
3.02
2.92
6.29
5.93
3.08
2.92

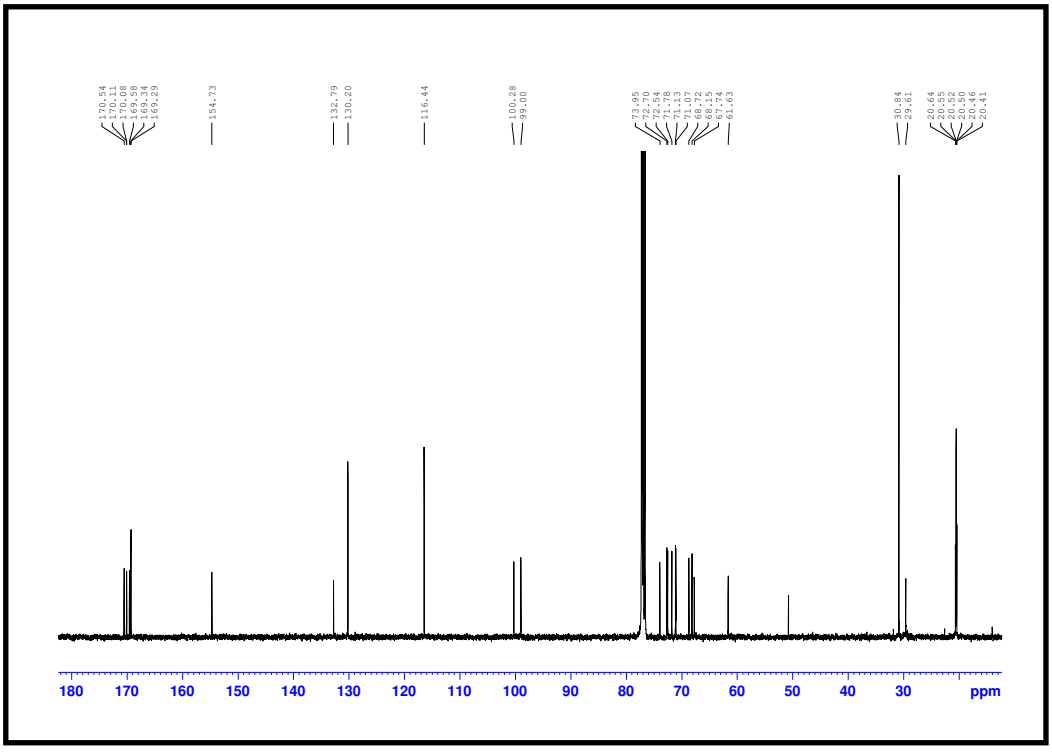
170.54
170.11
170.08
169.36
169.34
169.29
154.73
132.79
130.20
116.44
100.28
99.00
73.95
72.70
72.54
71.78
71.13
71.07
68.72
68.15
67.74
61.63
30.84
29.61
20.64
20.55
20.52
20.50
20.46
20.41
180
170
160
150
140
130
120
110
100
90
80
70
60
50
40
30
ppm

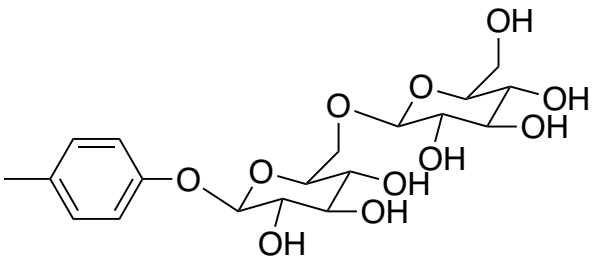
OH
O
OH
OH
O
OH
O
OH
OH
OH

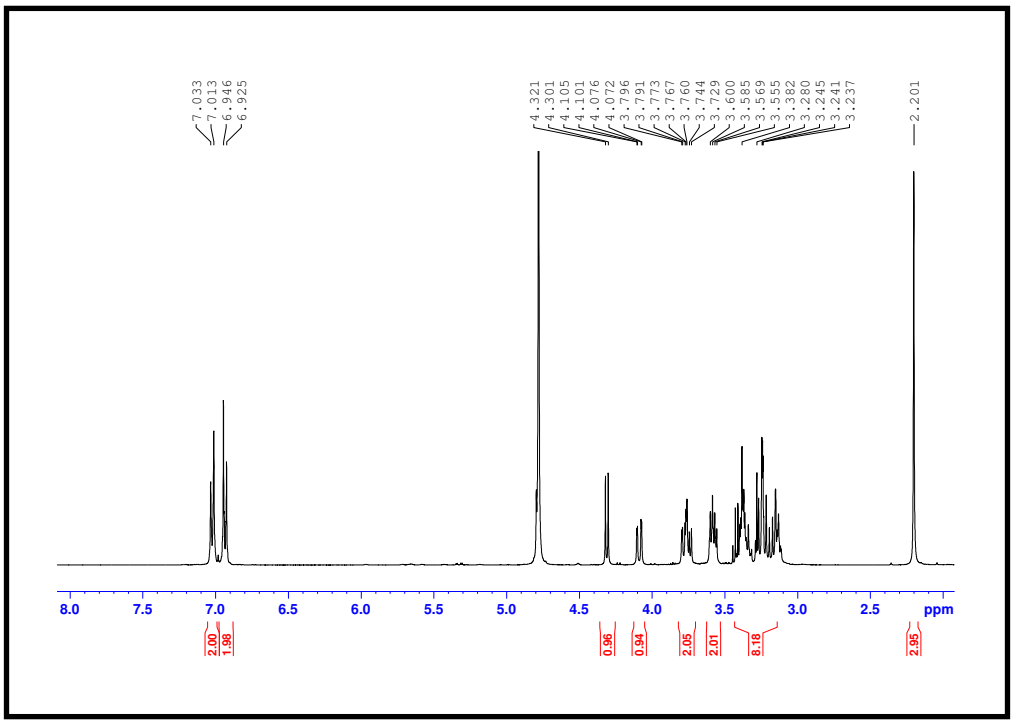
7.033
7.013
6.946
6.925
4.321
4.301
4.105
4.101
4.076
4.072
3.796
3.791
3.773
3.767
3.760
3.744
3.729
3.600
3.585
3.569
3.555
3.382
3.280
3.245
3.241
3.237
2.201
8.0
7.5
7.0
6.5
6.0
5.5
5.0
4.5
4.0
3.5
3.0
2.5
ppm
2.00
1.98
0.96
0.94
2.05
2.01
8.18
2.95

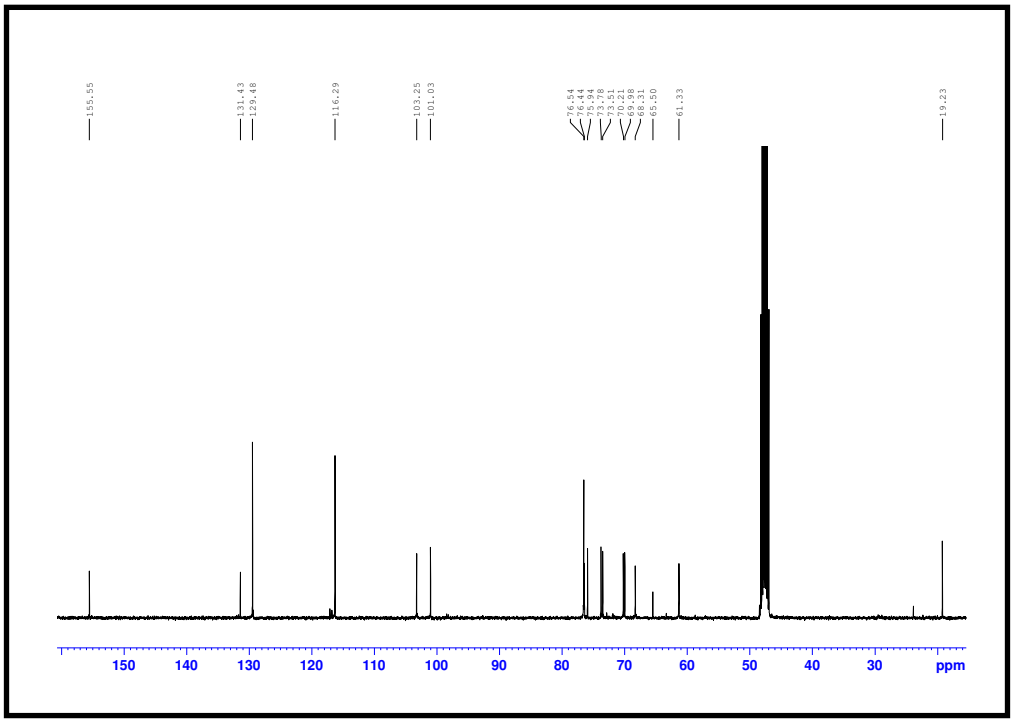
155.55
131.43
129.48
116.29
103.25
101.03
76.54
75.94
73.78
73.51
70.21
69.98
68.31
65.50
61.33
19.23
150
140
130
120
110
100
90
80
70
60
50
40
30
ppm